DANMARKS OG GRØNLANDS GEOLOGISKE UNDERSØGELSE **RAPPORT 2020/26**

Evaluation and risking of the seal capacity for CO2 storage in the Nini West Oil Field, Denmark

Project Greensand WP 4 TRL3

Niels H. Schovsbo

GEOLOGICAL SURVEY OF DENMARK AND GREENLAND
DANISH MINISTRY OF CLIMATE, ENERGY AND UTILITIES

G E U S

DANMARKS OG GRØNLANDS GEOLOGISKE UNDERSØGELSE **RAPPORT 2020/26**

Evaluation and risking of the seal capacity for CO2 storage in the Nini West Oil Field, Denmark

Project Greensand WP 4 TRL3

Niels H. Schovsbo

Confidential report

Copy No.

Released 01.10.2023

GEOLOGICAL SURVEY OF DENMARK AND GREENLAND
DANISH MINISTRY OF CLIMATE, ENERGY AND UTILITIES

G E U S

Table of Contents

SUMMARY AND MAIN CONCLUSIONS

The Nini West Oil Field is located in the Siri Canyon within the Danish North Sea. The canyon lies east of the Central Graben and extend from here and across the Ringkøbing-Fyn Basement High. The Siri Canyon formed in the Paleocene and feed a turbidity system that transported materiel from the Norwegian Stavanger Platform whereon glauconitic sand formed and to the Danish Central Graben. The turbidite system backstepped through the Palaeogene and deposited a series of isolated sand bodies imbedded in deep-water pelagic claystone within the Palaeocene-Eocene Rogaland Group (Våle to Balder Formation). The oldest of the sands are sealed by units within the Rogaland Group and the youngest sands are sealed by the above lying Eocene Horda and the Oligocene to Miocene Lark Formation that combined typically is one kilometre thick.

The Siri Canyon is characterised by overall low natural seismicity. The latest tectonic event that affected the North Sea area was the opening of the North Atlantic and as consequence ridge push forcers still affects Northern Europe. The primary seal to the Nini West Field is in the Nini-4 well 340 m thick and composed of shales that belong to the Eocene to Miocene Horda Formation and the lower to mid Lark Formation. The Horda Formation is characterised by greenish grey to greyish green fissile mudstone. Subordinate limestone benches and thin layers of black mudstones occur at some levels in the formation. The lower Lark Formation is dominated by dark, greenish grey, non-fissile mudstones with subordinate intervals of brownish grey mudstones. The secondary seal is in the Nini-4 well 550 m thick and belong to the mid to upper Lark Formation. This shale is composed by pale to dark brownish grey mudstones with subordinate intervals of greenish grey mudstones. The combined seal sequence is thus almost 900 m thick in the Nini West area. The above lying strata i.e. the remaining c. 800 m belongs to the Nolde Sand and the Nordland Group and is considered overburden.

During formation of the primary and secondary seal, smectite was the dominate clay mineral and due to the common mineralogical make-up of the shales the basic rock properties are very alike between the different shale formations as seen from analysis of the plasticity of the shales and the rock strength tests. Most of the variation appear to be related to the presence or absence of organic matter and/or radiolaria rich material that may or may not be present in all formations.

Measured shale porosities range between 15–25.8% for the lower Hordaland Group and measured transient brine permeability of the Sele Formation range between 1 and 20 nD pending on being orientation.

Rock mechanical tests have been performed on all shale formations expect the Lark Formation from where no core data within the Siri Canyon exist. The bulk of the tests were made on core material from the Sele and Lista Formations but also tests from the Horda Formation have been made. Unconfined compression strength (UCS) (measured and estimated) range between 8.1–13.3 MPa with the lowest value measured in the Sele

Formation and the highest value measured in the Lista Formation and with the Horda Formation as having an intermediate measured value (10.1 MPa).

We present a risk analysis for the seal capacity for the Nini West field seal complex following the risk factors presented by Bruno et al. (2014). The risk factors include 18 different parameters of which the current state of knowledge allows 12 to be evaluated here either with a reasonable certainty or provisionally pending on more data and analysis. The evaluation show that none of the evaluated parameters falls within the high-risk category of Bruno et al. (2014) and that most of the evaluated risk factors fall within the low to medium risk group. Most of the risk parameters that has been assigned a medium risk need, however, additional analysis and characterisation before final evaluation can be made. Compared to other seal complexes evaluated according to the Bruno et al. (2014) risk scheme, then the caprock capacity of the Nini West Field currently have a relative low risk score although not all risk factors have currently been evaluated.

Risk factor	Risk factor value ranges		
	High risk	**Moderate risk**	**Low risk**
Lateral extension of the storage zone/formation depth	< 25	25–100	> 100
Storage zone thickness/storage zone depth	> 0.5	0.1–0.5	< 0.1
Stress regime	Compressional	Transform	Extensional
Caprock strength	Weak	Moderate	Strong
Caprock thickness	≤ 3 m	3–30 m	≥ 30 m
Fault boundaries	Multiple	One	≥ 30 m
Natural seismicity	High	Moderate	Low
Number of caprocks	No	One	Multiple
Maximum formation pressure/formation depth	≥ 0.75	0.625–0.75	≤ 0.625
Desired maximum formation pressure/discovery pressure	≥ 1.5	1.25–1.5	≤ 1.25
Well density	> 15 km^2	5–15 km^2	< 5 km^2
Number of uncased wells/total number of wells	> 0.6	0.2–0.6	< 0.2
Temperature difference between the injected CO_2 and the ambient storage zone temperature	≥ 60°C	30–60 °C	≤ 30 °C
Caprock heterogeneity	Significant	Moderate	Strong
Caprock permeability	> $10^{-15} m^2$	10^{-18} – 10^{-15} m^2	< 10^{-18} m^2
Caprock lateral extend/storage zone thickness	< 25	25–100	> 100
Caprock dip	≥ 8°	2°–8°	≤ 2°
Minimum horizontal stress/vertical stress (stress ratio)	< 0.55	0.55–0.65	> 0.65

Risk scores for the caprock capacity of the Nini West Field. After Bruno et al. (2014). Green colour indicate that the risk factor has been evaluated with a reasonable confidence. Blue colour that the risk factor is only provisionally assessed here. Note that not all risk factors have currently been evaluated.

1.0 GEOLOGICAL SETTING

1.1 Introduction

Danish oil and gas fields are mostly composed of Cretaceous–Palaeocene Chalk and located in the Central Graben (DCG) (Fig. 1). The Siri Canyon that lies east of the DCG and extend from here and across the Ringkøbing-Fyn Basement High is one exception. In this canyon, a series of oil fields composed of glauconite rich sandstone of Palaeocene to Eocene age occur (Hamberg et al. 2005; Figs 1, 2, 3). The Siri Canyon formed in the Paleocene and feed a turbiditic system that transported materiel from the Norwegian Stavanger Platform whereon glauconitic sand formed and to the Danish Central Graben (Fig. 4). The sand turbidite system backstepped through the Palaeogene and deposited a series of isolated sand bodies imbedded in deep-water pelagic claystone belonging to the Palaeocene–Eocene Rogaland Group (Våle to Balder Formation (Fig. 5, Hamberg et al. 2005; Schiøler et al. 2007; Nielsen et al. 2015). The claystone formations are also seal for Danish Chalk fields and similar chalk fields in the Norwegian and UK part of the Central Graben. Additional seal capacity in the Siri Canyon stems from the above lying Eocene Horda Formation and the Oligocene to Miocene Lark Formation (Fig. 5) that combined typical is one kilometre thick (Schiøler et al. 2007). In the Siri Canyon post-depositional fluidisation led to local remobilisation of the sandstones and into the shales, which in some cases resulted in rather complex sandstone geometries (Hamberg et al. 2005, Svendsen et al. 2010).

In the DCG the main source rock is the Upper Jurassic to lowermost Cretaceous Farsund Formation (Damtofte et al. 1987, Schovsbo et al. 2020). The source rock was matured in the Palaeogene within the Tail End Graben (Fig. 2) and charged into the Siri Canyon from here (Ohm et al. 2006, Pedersen et al. 2016, Schovsbo et al. 2020). Ohm et al. (2006), however, points out that the charge was not continuous but aborted early and thus represent a “failed” migration route. The oil charge probably occurred before the late Paleogene i.e. within the last c. 5–10 Ma where the main expulsion from the Tail End Graben occurred (Schovsbo et al. 2020) as the oil in the Siri Canyon have an overall low maturity (Ohm et al. 2006). The oils show a mix with biogenic formed gas that probably results from microbial degradation of oil at rather shallow reservoir depth (Ohm et al. 2006, Svendsen et al. 2011).

The transition from chalk deposition to pelagic clays in the North Sea (Fig. 5) reflect a major palaeoceanographic and climatic change; the climate became cooler, and the breakup of the Atlantic Ocean shifted the major ocean currents in the proto North Atlantic Ocean. Because of the breakup, volcanic material such as basaltic tuffs and erosion produced from basalts produced smectite and montmorillonite rich clays that became and remained the dominant clay types of the Palaeogene successions in the North Sea until the Oligocene (Nielsen et al. 2015). Tuffs were also rock forming as seen in the Balder Formation (Fig. 5) that include very district tuff beds and is an easily identified formation within the North Sea and North

Atlantic Province (Schiøler et al. 2007). In the Palaeocene and Eocene, the sea deepened further and paleo-oceanographic and geochemical conditions favourable for diatomite blooms were meet. Therefore, radiolarian rich ooze also occurs with variably intensity in the claystone. Especially thick diatomite deposits located onshore Denmark are assigned to the Fur Formation (Schiøler et al. 2007).

The Siri Canyon Petroleum System was discovered in 1995 by drilling of the Siri-1 well (Hamberg et al. 2005) and since then four main field complexes composed of the Siri, Stine, Cecillie and Nini (the Nini West, Nini Main and Nini East) complexes have been put on production (Fig. 4). The fields are all operated by DONG Energy that is now part of INEOS E&P. The common geological setting of the fields including the common glauconite sand source area means that all fields were quite alike initially but due to differential diagenesis they have evolved slightly away from each other in terms of their porosity and permeability relationships and their chemically and mineralogically composition (Stokkendal et al. 2009; Weibel et al. 2010; Kazerouni et al. 2013).

1.2 Structural setting, stress, and present-day seismicity of the larger Siri Canyon Area

The Siri Canyon extends 120 km from the DCG in the West across the Ringkøbing Fyn High to the Danish-Norwegian Basin in the East (Figs 3 and 4). The area has a low natural seismicity as documented by GEUS that perform the national seismic survey of seismicity in Denmark. In Denmark natural seismic activity is mostly associate with the NW–SE trending Tornquist-Sorgenfrei Zone (Jensen et al. 2013; Voss et al. 2015; Gregersen et al. in press).

The latest tectonic event that affected the North Sea was the opening of the North Atlantic and as consequence ridge push forcers still affects Northern Europe (Arfai et al. 2018; Gregersen et al. in press). Data from the World Stress Map on the regional stress also show this (Fig. 7). However, the number of observations is limited for the Danish North Sea and the Siri Canyon as the only data are represented by a few break-out analyses of wells (c.f. Ask et al. 1996, Fig. 7). In the North Sea the maximum horizon stress (S_H) generally follow a NW–SE direction with local deviation typically induced by salt diapirs (Fig. 7).

1.21 Danish Earthquakes

For this report Tine Larsen, GEUS, has constructed a map that contains all Danish earthquakes recorded between 31st of October 1930 to 31st of July 2020 (Fig. 6). The earthquakes are registered on a minimum of three seismographs, and where the root-mean-square error on the location is at most 2.0s. The underlying data consists of manually read earthquake phases and amplitudes, and after c. 2000 also of digital waveforms. Between 1930 and 2000 the seismograms are primarily analogue. The hypocenters are calculated using data from the Danish National Seismograph Network supplemented by data from neighbouring countries, in particular Norway and Sweden.

The Danish earthquakes are relatively small and do not exceed 4.5ML in the North Sea. Small earthquakes are typically registered on a small number of seismographs with a lower signal-to-noise ratio than larger earthquakes. This translates into larger uncertainty on the hypocenter. For the North Sea earthquakes, the uncertainty is on the order of 20–50 km on latitude and longitude, and the depth is so poorly constrained, is often locked to a predefined depth of 15 km. When the registered event is known or suspected to be an explosion the depth is locked to 0 km.

Many explosions are registered in the Danish Territorial Waters. The seabed is still littered with unexploded mines from World War II, and the Danish Navy regularly searches for these mines and blow them away. In many cases GEUS is informed of these activities, but not consistently. Often a seismologist can discern an explosion from an earthquake by carefully inspecting the seismograms. This, however, still leaves events in the database that cannot with certainty be identified correctly. In case of doubt an event is left in the earthquake database. It is therefore likely, that some of the events in the North Sea currently categorized as earthquakes could be explosions.

The data quality does not permit to make a distinguish between natural earthquakes and induced/triggered earthquakes caused by activities in the oil and gas fields. It is noteworthy that most of the events near production fields happened in the 1980s and 1990s, especially as the detection capability has increased significantly since then. A few earthquakes have been felt strongly on the drilling rigs. Furthermore, most of the North Sea events occurring outside of the known earthquake zone bordering Skagerrak, occur during regular working hours (i.e. 8–19 UTC). As natural earthquakes are equally likely throughout the day and night, this information could indicate that the North Sea events are a mixture of explosions, induced/triggered events, and natural earthquakes.

1.3. Lithostratigraphy in the Siri Canyon

There has over the years been developed an extensive and detailed lithostratigraphy for the Paleogene to Neogene succession in the North Sea as the shales form very extensive and easy correlatedly units across long distances (Fig. 5). The lithostratigraphy adopted here for the Palaeocene to Eocene is from Schiøler et al. (2007) that also presented a review of the succession in the North Sea and onshore Denmark, isochore maps of the main units and regional well correlations panels in addition to sedimentological descriptions and biostratigraphical age determinations. For younger successions we follow descriptions from the North Sea as presented in the Millennium Atlas Chapter 16.

In the following a summary of the main lithological characteristics and definitions of the shale formations (Fig. 5) are presented:

Rogaland Group

The Rogaland Group comprises the Paleocene to lower Eocene marlstone and mudstone succession between the top of the Ekofisk Formation of the Chalk Group and the mudstones of the Hordaland Group in the central North Sea. In most of the Danish sector, the Rogaland Group has a relatively uniform thickness and comprises the Våle, Lista, Sele and Balder Formations. Sandstone units in the Rogaland Group include Ty, Heimdal and Hermod Formations (Fig. 5).

Våle Formation

Marls with interbedded claystones, limestones and silt- and sandstone stringers that overlie the Chalk Group in the central and northern North Sea. The lithology is dominantly light grey to greenish grey, heavily bioturbated pyrite-bearing marlstones. Thin sandstone intrusions are present locally. In the Siri Canyon, the marls are interbedded with turbidite sandstones.

Depositional environment. Over most of the Danish sector, the marlstones of the Våle Formation comprise hemipelagic deposits and deposits from dilute turbidity currents. The marlstones are probably largely of turbiditic origin.

Log characteristics. From its base to its top, the Våle Formation is characterised by an overall steady increase in gamma-ray response, combined with an overall steady decrease in sonic readings. When the Bor Member sandstones are present, blocky log signatures with higher gamma-ray values and lower sonic readings interrupt this general trend.

Lista Formation

The Lista Formation is a widespread, non-laminated mudstones that overlie the marls of the Våle Formation. The Lista Formation is subdivided into six members. Three of these, the Vile, Ve and Bue Members, are mudstone units that have widespread distribution in the North Sea and can be correlated with Danish onshore units.

Distribution and thickness. The Lista Formation is present throughout the North Sea, except in a few areas where it has been removed by erosion. In the Danish sector, its thickness varies from 0 to 108 m.

Lithology. The formation is characterised by dark coloured, predominantly greyish, greenish, or brownish, non-laminated to faintly laminated, non-calcareous mudstones. The Lista Formation is predominantly non-tuffaceous but becomes tuffaceous towards its top. In the Siri Canyon, glaucony-rich, massive sandstone layers and injected sandstone bodies occur in the Lista Formation.

Depositional environment. The Lista Formation consists predominantly of hemipelagic mudstones and was probably deposited from very dilute turbidity currents and from suspension. The composition of the microfaunal assemblage indicates a relatively open marine depositional setting in upper to possibly middle bathyal depths with oxic to dysoxic bottom conditions.

Log characteristics. Although fluctuating, both the gamma-ray and sonic log readings in the Lista Formation have higher mean values than those of the underlying Våle Formation and lower mean values than those of the overlying Sele Formation. In wells where mudstone facies dominate in the Lista Formation, the gamma-ray and sonic log patterns can be subdivided into three that reflects the succession of three different mudstone units, established as members by Schiøler et al. (2007).

Sele Formation

The Sele Formation represent dark grey to greenish grey, laminated and carbonaceous, tuffaceous, montmorillonite-rich shales and siltstones that overlie the non-laminated and non-tuffaceous shales of the Lista Formation in some areas, or arenaceous sediments belonging to a variety of different units in other areas. The base of the Sele Formation is located at the base of the “laminated tuffaceous shales” that overlie the “non-laminated, non-tuffaceous shales” of the Lista Formation. Sandstones occur in the Sele Formation in the Danish sector are termed Kolga Member (Fig. 5).

Subdivision. The Sele Formation is informal threefold subdivided based on the gamma-ray log signature.

Distribution and thickness. The Sele Formation is recognised from many North Sea wells and it has a basinwide distribution. In the Danish sector, the thickness varies from 5 to 54 m.

Lithology. The Sele Formation consists of medium to dark grey, brownish, or black laminated mudstones. Thin tuff layers occur in the upper part of the formation. It contains three or more well-laminated intervals where dark mudstone beds alternate with lighter coloured mudstone beds. The well-laminated intervals are enriched in organic material resulting in a high gamma-ray response, primarily due to increased uranium content. The most organic-rich, and often darkest, most well-laminated interval is found in the basal part of the formation. The mudstones of the Sele Formation show an overall upward increase in the silt fraction. In the upper half of the formation, the mudstones may be interbedded with thin, very fine-grained sandstone laminae and thin sandstone beds. The sandstone beds are up to 12 cm thick, normally graded and display parallel lamination. Locally, and dominantly in the upper part of the formation, graded tuff laminae less than 1 cm thick are present. In cores, the tuff laminae have a light purple colour. Small calcite concretions are present, but rare. In the Siri Canyon, the Sele Formation is interbedded with sandstones or it grades upwards into a succession of thinly interbedded sandstones and mudstones. Thin sandstone intrusions occur, but only in the lower part of the formation.

Depositional environment. The mudstones of the Sele Formation represent a mixture of pelagic fallout and dilute, low-density mud turbidites. The well-laminated character of the sediment, the high content of organic material and uranium, and the general lack of trace fossils and benthic foraminifers indicate starved sedimentation under dysoxic to anoxic bottom conditions. Common diatoms indicate a high nutrient level in the water mass. The tuffs of the Sele Formation are evidence of extensive volcanism in the region. Based on microfossils, the palaeo-environment has been suggested to represent an upper bathyal setting with a depth estimate of around 300 m. The palynomorph assemblage indicates a marine environment characterised by a massive influx of terrestrial palynomorphs.

Log characteristics. The Sele Formation is characterised by high gamma-ray readings throughout, with several gamma-ray peaks. On the gamma-ray log, the base of the Sele Formation is generally marked by a conspicuous upward shift to consistently higher gamma-ray readings than those of the underlying member. In most wells, a pronounced gamma-ray peak follows a short distance above the base of the Sele Formation. In wells to the north and west of the Danish sector, the stratigraphic distance between the shift to higher gamma-ray readings at the base of the Sele Formation and the gamma-ray peak is considerably greater. In most Siri Canyon wells, the basal high gamma-ray interval is missing, and the base of the Sele Formation is marked by the pronounced gamma-ray peak (e.g. the Nini-3 well, Fig. 8).

Balder Formation

The Balder Formation represent variegated, fissile, and laminated shales with interbedded tuff layers that lie between the Sele and Horda Formations.

Distribution and thickness. The Balder Formation extends over most of the central and northern North Sea. In the Danish sector, it reaches a thickness of more than 20 m in the Siri Canyon and on the western part of the Ringkøbing–Fyn High (Fig. 2) and in the northern part of the Danish Central Graben. The Balder Formation thins to less than 5 m towards the south-west and to less than 10 m in the eastern part of the Danish part of the North Sea.

Lithology. The Balder Formation is composed of laminated, dominantly grey, fissile shales with interbedded dark and light grey, purple, buff, and green sandy tuffs. The tuffs are normally graded and less than 5 cm thick. Locally the tuff beds are slumped. Sandstone beds, interpreted as intrusive sandstone bodies, occur locally in the Balder Formation.

Depositional environment. A restricted marine palaeoenvironment at upper bathyal depths with dysoxic to anoxic bottom conditions is suggested for the Balder Formation by Schiøler (2007). This is based on the scarcity of calcareous microfossils and agglutinated foraminifers combined with common to abundant siliceous microfossils, especially diatoms.

Log characteristics. The Balder Formation is characterised by a relatively high gamma-ray values in its lower and higher parts but shows low values in its middle part (Fig. 9). The change in gamma-ray response is normally gradual, but relatively steep. The gamma-ray motif is mirrored by a gradual increase in sonic readings commencing at the formation base, culminating at or slightly below the level of minimum gamma-ray values in the middle part of the formation, followed by a gradual decrease towards the top cm of the formation where the lowest sonic reading is reached.

Hordaland Group:

Horda Formation

The Horda Formation (lower to upper Eocene) is composed of a greenish grey basinal mudstone that overlies the grey tuffaceous mudstones of the Balder Formation and underlies the greenish grey to brown mudstones of the Lark Formation.

Distribution and thickness. The Horda Formation extends over the central and northern North Sea and is present in all wells in the Danish sector of the North Sea. The Horda Formation reaches a thickness of 906 m in the Central Graben well Tordenskjold-1, but thins towards the east and south-east to less than 100 m, with minimum recorded thicknesses of 9 m in the Ida-1 well and 4 m in the S-1 well (see Fig. 2 for location). An isochore map of the Horda Formation is shown in Fig. 10.

Lithology. The Horda Formation is characterised by greenish grey to greyish green fissile mudstone. Subordinate limestone benches and thin layers of black mudstones occur at some levels in the formation. In many wells the lowermost 20–50 m of the Horda Formation consists of red-brown mudstones.

Log characteristics. The Horda Formation is characterised by an overall stable gamma-ray and sonic log motif with a lower gamma-ray response than that displayed by the underlying Balder Formation and the overlying Lark Formation (Fig. 9). In a few wells, the base of the Horda Formation shows relatively high gamma-ray values, which decrease to lower and more stable values over a short interval. The sonic readings decrease slightly upwards from the base to the top of the Horda Formation.

Lark Formation

The Lark Formation (upper Eocene to mid Miocene) represent a brownish grey mudstone-dominated lithofacies (Fig. 5) that overlies the more variable association of red and green-grey mudstones, silty mudstones and sandstones of the Horda Formation and underlies the grey, sandy and shelly mudstones, siltstones and sandstones of the Nordland Group.

Distribution and thickness. The Lark Formation extends over the central and northern North Sea and is probably present in the entire Danish sector of the North Sea. Its depocenter is in the central and northern part of the Danish sector, along the eastern boundary of the Danish Central Graben, where it reaches a thickness of 1194 m in the Siri-3 well (Fig. 11). The Lark Formation thins west to a thickness of 389 m in the Tordenskjold-1 well in the Central Graben, and east to a thickness of 240 m in the S-1 well on the Ringkøbing–Fyn High (Fig. 11).

Lithology. The lower Lark Formation (L1–3, see Fig. 9) is dominated by dark, greenish grey, non-fissile mudstones in most wells; in some wells subordinate intervals of brownish grey mudstones are also present. Thin layers of white or reddish-brown carbonate are also recorded in the upper levels of the lower Lark Formation. The upper Lark Formation (L4, see Fig. 9) is dominated by pale to dark brownish grey mudstones with subordinate intervals of greenish grey mudstones in its lower levels. The uppermost 50–100 m of the formation consists of yellowish grey to light brown mudstones. In eastern and northern parts of the Danish sector, discrete sandstone interbeds and thin sandstone stringers occur throughout the formation.

Log characteristics. The lower part of the Lark Formation is characterised by an overall stable gamma-ray log signature, whereas the upper part of the formation has a more unstable signature (Fig. 9). This change in gamma-ray log signature coincides approximately with the change from lithologies dominated by greenish grey mudstones to lithologies dominated by dark to light brownish grey mudstones at the base of unit L4 (Fig. 9).

Nordland Group

In the North Sea the Nordland Group (mid Miocene to recent) is dominated by marine claystones. In the Norwegian in the Viking Graben area the sandy Utsira Formation occurs in the lower part of the group. The uppermost part of the group consists of unconsolidated clays and sands with glacial deposits uppermost. In the Siri canyon the lower Nordland Group also include sandy beds and thicker units (Millennium Atlas Chapter 16 2001, Nielsen et al. 2015).

Distribution and thickness. The base of the group occurs at the passage from the generally brown shales of the Lark Fm into the more massive and blockier, generally grey, claystones of the Nordland Group. This contact is usually marked by a break on the logs which represents an unconformity of early to middle Miocene age. The lower boundary is normally at the base of the sandy unit. In this case the contact is marked by a decrease in gamma-ray readings from the claystones of the Lark Formation into the sand. Where the basal part of the Nordland Group is developed as claystone the boundary is placed at log breaks associated with a change in claystone colour.

Lithology. The grey, sometimes greenish-grey and grey-brown mudstones that are soft, locally silty, and micaceous. Deposited in open marine, with glacial deposits in the upper part in some areas.

2.0 THE SEAL UNIT COMPLEX AND OVERBURDEN IN NINI WEST FIELD AREA

Exploration and development wells drilled in the Nini field complex provide the lithological description of the reservoir and of the seal and overburden rocks presented here. In the description the gamma-ray and the resistivity wire-line logs provide supplementary information on the lithology and indications of the porosity and fluid type in the sandy units.

In general, the top section of the wells was drilled with no to limited returns to the surface thus limiting the description of this interval. For deeper sections cutting descriptions were made routinely and samples hereof were picked with c. 10 or 5 m interval. These samples are now kept at the GEUS core repository and are available for inspection and re-sampling. A full wire-line log suite was typically only acquired in the reservoir section allowing for a detailed analysis to be made here. The sections above the reservoir only have a limited wire-log suite recorded. A full list of logs available in each well pr. log run have not been made for this report.

2.1 Seal and overburden lithology variation in the Nini west field area

Released final well reports (FWR) of all exploration and appraisal wells drilled within the Danish Territory are available to the public via the GEUS Frisbee web page (http://frisbee.geus.dk/). Below is presented a lithological overview of the seal and overburden rock in the Nini West area based on the description from the Nini-4/4A well FWR. For more detailed cuttings description and for full core descriptions see the FWR and the core description report (DONG 2003).

In Fig. 12 the lithostratigraphic units drilled in the Nini-4 wells are show together with the gamma-ray and deep resistivity logs. The log based stratigraphical division follows Schiøler et al. (2007). The subdivisions on the Lark Formation for the Mona-1 well presented in Fig. 9 have thus been used as reference for the Nini-4 log stratigraphical division. Below is the lithologies within the different lithostratigraphic units detailed.

Lithologies in the Nini-4 well:

Nordland Group; recent to late Miocene: 143.4-509.6 m (105.6-471.8 m TVDMSL)

During driving and drilling of the 30" conductor returns to the rig deck were loose sand.

The Quaternary is mainly quartz *sand*. The sand is loose. Grains are colourless and clear to translucent, occasionally opaque, medium to coarse, very coarse in parts. They are subangular to subrounded and moderately well sorted. The sand contains rare shell fragments and common dark brown to black lignite.

Traces of lithic rock fragments and micro pyrite are seen. In places the sand is interbedded with grey, soft and amorphous *clay*.

Sand is still the dominant lithology in the upper part of the pre-Quaternary section (179.6-509.6 m). The quartz sand is loose, colourless, and clear to translucent grains, occasionally opaque, fine to medium to coarse. Subangular to rounded and poorly to moderately sorted. The sand is partly slightly silty and contains traces of glauconite and of shell fragments and of lithic rock fragments (quartz, claystone and volcanics). It has good traces of mica and lignite.

Clay/claystone occurs as beds in the sand and becomes the dominant lithology downwards. The clay is light to medium grey or greyish brown. It is very soft, amorphous, and sticky and in places slightly silty. It is non-calcareous. Between 200 m and 510 m, the soft clay/claystone was washed away in the mud. Therefore, only scattered cuttings descriptions are available from this interval.

Hordaland Group; Early Miocene **-** Early Eocene**:** 509.6–1784.8 m (471.8–1747.0 m TVDMSL)
The Hordaland Group comprises the following lithostratigraphic units:
Nolde Sand Formation
Lark Formation
Horda Formation with injected Frigg Sand Member.

Nolde Sand Formation: Late Oligocene: 648.7–762.8 m (610.9–725.0 m TVDMSL).
The Nolde Sand Formation consists of sand/sandstone with claystone interbeds and is characterized by low GR and resistivity readings in the sand dominated intervals. The *sand/sandstone* is colourless. In places the sandstone has a weak, pale orange carbonate cement/matrix. It is fine- to medium-grained, occasionally coarse-grained. It consists of clear, occasionally opaque quartz grains which are subangular to well-rounded and poorly sorted. The sandstone has abundant glauconite clasts, common shell fragments and foraminiferous microfossils, traces of pyrite and is commonly micaceous. The *claystone* is dark greyish brown, moderately soft, blocky, silty, commonly micaceous, non-calcareous and has earthy texture.

Lark Formation: Oligocene–Middle Eocene: 762.8–1701.8 m (725.0–1664 m TVDMSL).
The Hordaland Group comprises mainly claystone, containing stringers of limestone that become increasingly frequent towards the base of the unit. A few sandstone beds are seen. The *claystone* is brownish grey to grey, occasionally very light greenish brown. Downwards, they become medium brown to greyish brown or light brown, occasionally dark brown, yellowish brown olive grey, or greenish grey. The claystones are very soft to firm. They are subblocky to blocky and occasionally amorphous or sticky. The claystones

have earthy texture, lightly silty to silty and sandy parts occur, grading to argillaceous *siltstone* and *sandstone*. The claystones become micro-micaceous downwards and they are non- to slightly calcareous. Locally, the claystones are glauconitic. Traces of pyrite occur in places. The *limestones* are white to very light grey, dark yellowish orange, or light brown to dark yellowish brown. They are firm, occasionally soft or hard, and are occasionally granular with colourless calcite grains in white matrix. Glauconite inclusions occur occasionally. The limestones are sub-blocky to blocky or amorphous, occasionally angular.
Between 1380 – 1430 m two sandy intervals occur. The sand is very pale brown to brown with glauconite. Both sands grades into siltstone/claystone.

Horda Formation: Middle–Early Eocene: 1701.8–1784.8 m (1664.0–1747.0 m TVDMSL)
The Horda Formation also comprises the Frigg injected Sand. Apart from the sandstone member it consists of claystone with a few limestone stringers like those seen higher up in the Hordaland Group.

The *claystone* is predominantly pale greenish grey, commonly pale green, becoming darker downwards. It is moderately soft becoming hard, is blocky to sub-platy or sub-fissile and slightly micro-micaceous. Locally, it is silty or has dark green glauconitic staining or fine pyrite aggregates. Commonly it is tuffaceous: bluish green with fine, white, or pale green inclusions. The claystone is non-calcareous.

Frigg Sand Member: Early Eocene: 1771.9–1781.9 m (1734.1–1744.1 m TVDMSL)
The top of the Frigg Sand Member is recognized by a distinct downward increase in resistivity readings in response to the oil content in the unit. The unit is made up of *sandstone* consisting of clear, pale orange or pale brown, translucent quartz grains with abundant dark brown to black *glauconite* (up to 50 %). The grains are fine, well sorted and subangular to subrounded. The sandstone is friable with weak, partly silty cement and traces of mica.

Rogaland Group: Early Eocene–Late Palaeocene: 1784.8–1856.9 m (1747.0–1819.1 m TVDMSL)
The Rogaland Group comprises the following lithostratigraphic units:
Balder Formation
Sele Formation
Lista Formation

Balder Formation: Early Eocene: 1784.8–1788.8 m (1747.0–1751.0 m TVDMSL)
The top of the Balder Formation is picked at slight downhole increases in sonic velocity and density and a distinct decrease in resistivity. The formation consists of claystone with beds of tuff (volcanic ash). The *claystone* is light to medium grey or brownish grey. It is hard and blocky and has traces of fossil fragments.

Occasionally, the claystone grades into argillaceous *limestone*. The *tuff* is greyish to bluish green, pale green, or very light grey. The texture is finely granular, and the tuff has irregular fractures and traces of pyrite.

Frigg Sand injected into Horda and Balder Formations (Reservoir)
Frigg Sand injected into the basal Horda Formation and upper Balder Formation obscures the transition between the Hordaland and Rogaland Groups. The *sandstone* is dark greyish green and made up of very fine- to fine-grained quartz and *glauconite*. It is tuffaceous, argillaceous, slightly calcareous and has traces of microfossils.

Sele Formation: Late Palaeocene: 1788.8–1795.0 m (1751.0–1757.2 m TVDMSL)
Claystone makes up the Sele Formation. The top of the formation is marked by a distinct downhole GR increase. The *claystone* is medium to greyish brown. It is hard, has subconchoidal fracture and is micro-laminated. It is silty and commonly micaceous. It has traces of fossil fragments and is non-calcareous.

Lista Formation: Late Palaeocene: 1795.0–1804.6 m (1757.2–1766.8 m TVDMSL)
Claystone makes up the Lista Formation. The top of the formation is marked by a distinct downhole GR decrease. The *claystone* is greyish green. It is occasionally sub-fissile. It is tuffaceous in places, micaceous and non-calcareous.

2.2 Well correlation in the Nini area

The detailed wire-line log stratigraphy for the Paleocene to recent sedimentary succession in the North Sea (c.f. Schiøler et al. 2007) allow for a very detailed correlation to be made across the Nini Field Complex as seen from the profile presented in Fig. 13 that extends from the Nini-4 well in SW to the Nini-3 well in NE i.e. approximately 12 km (Fig. 4). In the correlation all lithostratigraphic units have been identified; the Horda Formation and the mid Lark Formation (L–2) thins from SW to NE whereas the other units show almost the same thickness between the wells. The correlation documents the lateral extend of the units as their log signature directly can be compared to the regional correlation profiles presented by Schiøler et al. (2007) as outlined above. The log-stratigraphy thus provides a high confidence level in stratigraphical and lithological make-up of the succession.

The thickening of the Lark Formation (L2) towards SW i.e. in the Nini-2 and Nini 4 wells in Fig. 13 is partly related to the presence of sandy beds here that can be correlated between the Nini-2 and Nini-4 wells but not to the Nini-3 and Nini-5 wells (Fig. 13). The sandy beds in the Nini-4 well are tentative interpreted as related to turbiditic sandstone body of a limited size. The permeability and porosity of the sands have not been quantified but judged from the conductive nature of the beds they appear water saturated (low resistivity response is recorded in the deep resistivity log across the beds c.f. Fig. 12) and is thus inferred to be porous. Also, the lithological description for the interval appears to exclude cemented beds (see above).

2.3 The Nini West Seal Complex

The immediate seal to the Nini Field Complex is the shales belonging to Sele and Balder Formation in the Rogaland Group, as the age of the sandstones within the different parts of Nini Field Complex varies slightly; the youngest sand are capped by the Balder Formation and the older sands are capped by the Sele Formation (Fig. 13). In addition to these formations the primary seal include the shales that belong to the Horda and Lark Formation. This combined seal sequence thus range in thickness from 340 m in the Nini-4 and to c. 900 m in the Nini-3 well. The reason why the primary seal is lower in the Nini-4 well is that the porous sand beds (between 1380 – 1430 m) in the mid Lark Formation (Fig. 12) is considered the boundary between the primary (1772 – 1430 m, 340 m thick) and the secondary seal (1380 – 830 m, 550 m thick) in the Nini-4 well. The above lying strata in the Nini-4 i.e. the remaining c. 800 m of strata that belons to the Nolde Sand and the Nordland Group (830 m – to seabed) and thus succession is considered overburden.

Seismic imaging of the seal complex and fault mapping of the seal and overburden within the Nini Field Complex are presented in the Project Greensand Phase 1 - Feasibility Report (2020). These sections do not appear to show evidences of leaks such as gas chimneys atop of the Nini West Field. Other evidences that suggest that leaks are limited not only from the Nini West Field but in the entire Siri Canyon System stems from bright spot mapping conducted in the North Sea area (Fig. 14). Bright spots are one of several Direct Hydrocarbon Indicators (DHI) and are presence above most known oil or gas fields where they indicate either the presence of leaked gas from below and/or the presence of shallow biogenic gas. In general, the oil and gas fields in the DCG are characterised by the presence of this DHI type (compare Figs 1 and 14). The notable exception is the Siri Canyon that is located within an area of low bright spot activity despite the location of the known oil fields below. This suggests that gas is not leaking or leaking to a much lower extends that the fields in the DCG.

3.0 CHARACTERIZATION OF THE NINI SEAL COMPLEX

As part of the Project Greensand, 20 samples for chemical and mineralogical characterisation of the seal section are currently being processed. The samples are picked from the Hordaland to lower Lark Formation interval in the Nini-4 and 4A and represent both core and cuttings material. The analytical program includes determination of the elemental composition and mineralogy, porosity, surface area determination (BET) and

Hg injection experiments (MICP). Since the results from these analysis are not available currently, they will be included in a later and updated version of the assessment of the seal capacity in the Nini West.

3.1 Data and sample availability

The Palaeogene shales are all sensitive to water as they swell and advanced studies to mitigate this drill hazard have been made by the operator during the last 15 years (Geo 2005; Nes et al. 2009; Core Laboratories 2014). These studies are the main source of data on the seal and have been used extensively in preparation of this part of the report.

The tests made in the above-mentioned reports have all been performed on preserved core material from newly drilled wells as the shales are sensitive to storage conditions notably to dry-out effects. Despite using such material, the report prepared by Geo (2005) specifically mention that even this fresh and preserved material are very sensitive to treatment and that the part of the material quickly damage. The other two reports only sporadic mention the sample condition as problematic.

The report by Geo analyse a broad range of formations and include samples from the Na-2P (unknown drill date assumed 2002), Vivi-1 (drilled 2004), SCB-1X (unknown drill date assumed 2003), Siri-5 (drilled 2002), Cecilie-2 (drilled 2002) and the Sofie-1 (drilled 2003) wells and thus analysis were performed on material that was between 1–3 year old. The report by Sintef (Nes et al. 2009) include core samples from the Sele Formation in the Nini-5 well (drilled in 2007). The report by Core Laboratory (2014) analysed Palaeocene shale samples from the Solort-2 well (drilled 2013) i.e. on core samples that were less than one year old.

The above cited studies thus all analyse relative fresh shale samples compared to any similar studies that could be commissioned on material from the Siri Canyon today. Also, at present only a very limited amount of preserved cap rock samples exists and even these are now quite old, i.e. the preserved samples in the Nini-4 well (drilled in 2002). Therefore, it is questionable if additional advanced core studies such as rock mechanical or other advanced testing can produce reliable results with the current available material.

3.2. Cores and sedimentology

Due to the slight variation in stratigraphy of the Siri Canyon reservoirs most of the cores have been cut in the Lista and Sele Formations i.e. at stratigraphical levels slightly older than the Nini West reservoir that represent one of the youngest stratigraphical intervals in the canyon. The lower part of the primary seal in the Nini West has been cored in the Nini-4 and Nini-4A wells and core descriptions have been made and presented in Dong (2003) and by Humphrey & Lucas (2003).

In the Nini-4 well the Horda Formation is described as a dark grey to reddish brown laminated mudstone with occasionally high tuffaceous content (Fig. 15). There are also sections with high content of radiolaria that can be identified on gamma ray log as intervals with low response (c.f. Fig. 12). The radiolaria are pyritised, cemented by zeolite and replaced by cristobalite. In the Horda Formation there are moderately to heavily bioturbated intervals interbedded with non-bioturbated parts. The lowermost 5 m of the Horda Formation are light grey or greenish grey in colour. It is weakly bioturbated but only a few *Helminthopsis* could be identified by Humphrey & Lucas (2003). The lower boundary to the reservoir, the Frigg sand, is sharp, but not regular. No *in situ* sand layers are recognized in the Horda Formation.

3.3 Mineralogy and clay types of cap rock in the Siri Canyon

Mineralogical analysis of the shales from the primary seal have been made in the Nini-4 and 4A cored sections (Table 1 and 2). The Horda Formation is here composed of more than 60% clays and about 20% quartz. Of the clay minerals more than 60% is composed by illite/smectite followed in abundance by illite/mica and then by chlorite and zeolite (Table 1). Low amount to no carbonate minerals were observed and potentially reactive minerals such as K-feldspar and plagioclase constitute together less than 10% of the bulk rock composition (Table 1). The clay size fraction of the samples constitutes about 75–80% by weight testifying to the fine-grained nature of the rock (Table 2). Domination of illite/smectite is also seen in the clay size fraction where also glauconite and chlorite have been detected both constituting minor fractions (Table 2).

Nes et al. (2009) also reported the mineralogical composition from two samples in the Sele Formation from the Nini-5 well (not shown their table 3.1). The shale sample had a mineralogical composition similar to those presented from the Nini-4 well with smectite as the dominant mineral. The other sample was picked from radiolarian rick interval and proved to contain mostly of opal.

Table 1 Bulk mineralogy of samples from the Nini-4 and 4A wells. The cap rock analyses are represented by the interval 1746.2–1766.46 m. From Humphrey & Lucas (2003).

XRD No.	Well	Depth(m)	Illite/Smec	Illite+Mica	Glauconite	Chlorite	Zeolite	Chert*	Quartz	K Feldspar	Plagioclase	Calcite	Mg-Calcite	Dolomite	Siderite	Pyrite	Haematite	Anatase
167	Nini-4	1746,20	33,6	23,7	0,0	4,3	0,0	0,0	24,5	0,0	9,1	2,2	0,0	0,0	0,0	0,0	2,6	0,0
168	Nini-4	1746,41	29,3	26,8	0,0	6,9	0,0	0,0	24,0	0,0	10,5	0,0	0,0	0,0	0,0	2,3	0,0	0,0
169	Nini-4	1749,09	39,3	20,1	0,0	6,8	9,1	0,0	17,7	2,5	2,6	0,0	0,0	0,0	0,0	2,0	0,0	0,0
170	Nini-4	1749,52	40,7	17,4	0,0	5,0	9,1	0,0	20,5	3,4	2,6	0,0	0,0	0,0	0,0	1,4	0,0	0,0
171	Nini-4	1757,20	37,0	16,9	0,0	2,8	10,5	0,0	16,8	5,0	4,0	0,0	0,0	0,0	0,0	7,0	0,0	0,0
172	Nini-4	1762,20	34,4	17,4	0,0	2,5	11,9	0,0	20,5	3,9	3,3	0,0	0,0	0,0	0,0	6,1	0,0	0,0
173	Nini-4	1766,41	13,8	6,9	0,0	0,0	0,0	59,3	11,2	TR	1,8	0,0	0,0	0,0	0,0	7,0	0,0	0,0
174	Nini-4	1766,46	16,3	6,0	0,0	0,0	0,0	57,2	11,6	TR	1,8	0,0	0,0	0,0	0,0	7,1	0,0	0,0
175	Nini-4	1771,04	5,0	6,9	14,3	1,0	0,0	0,0	62,4	4,5	2,0	0,6	0,0	1,0	2,4	0,0	0,0	0,0
176	Nini-4	1774,03	4,5	7,4	12,9	1,2	0,0	0,0	62,1	7,7	2,5	TR	0,0	0,0	1,1	0,6	0,0	0,0
177	Nini-4	1777,04	1,5	7,3	11,9	1,8	0,0	0,0	68,6	4,2	2,1	0,0	0,0	0,0	2,7	0,0	0,0	0,0
178	Nini-4	1780,04	1,4	9,1	12,9	1,6	0,0	0,0	65,3	4,0	4,5	0,0	0,0	0,0	1,3	0,0	0,0	0,0
179	Nini-4	1783,12	1,4	10,8	10,4	1,1	0,0	0,0	56,2	6,5	3,3	1,1	0,0	0,6	8,7	0,0	0,0	0,0
180	Nini-4	1783,81	32,9	3,8	0,0	3,2	0,0	0,0	16,9	0,0	20,8	4,3	0,0	0,0	5,4	3,1	0,0	9,7
181	Nini-4	1788,56	6,9	12,6	0,0	4,6	19,7	0,0	35,8	0,0	2,3	0,0	0,0	0,0	0,0	18,3	0,0	0,0
182	Nini-4	1788,76	10,1	15,1	0,0	2,4	17,6	0,0	34,2	2,9	2,1	0,0	0,0	0,0	0,0	15,7	0,0	0,0
183	Nini-4	1852,11	2,5	8,6	11,5	1,3	0,0	0,0	62,8	9,7	1,9	0,0	0,0	0,0	1,1	0,6	0,0	0,0
184	Nini-4	1856,10	7,0	9,0	23,9	1,4	0,0	0,0	54,4	3,0	1,4	TR	0,0	0,0	0,0	0,0	0,0	0,0
185	Nini-4A	1928,20	17,3	7,6	0,0	4,2	0,0	48,7	13,6	TR	2,0	0,0	0,0	0,0	0,0	6,5	0,0	0,0
186	Nini-4A	1932,50	4,4	7,2	14,7	2,1	0,0	0,0	60,1	5,5	1,9	1,0	0,0	1,0	1,9	0,0	0,0	0,0
187	Nini-4A	1935,50	4,0	7,8	12,5	1,6	0,0	0,0	66,6	3,1	2,0	0,0	0,0	0,0	2,4	0,0	0,0	0,0
188	Nini-4A	1938,50	3,4	7,7	15,0	2,4	0,0	0,0	61,4	3,1	1,5	0,0	0,0	1,5	3,9	0,0	0,0	0,0
189	Nini-4A	1941,50	2,9	7,5	13,1	2,6	0,0	0,0	62,5	3,6	3,5	0,0	0,0	0,8	3,4	0,0	0,0	0,0
190	Nini-4A	1944,50	3,1	6,7	12,0	2,6	0,0	0,0	67,1	3,0	1,3	0,0	0,0	0,0	4,1	0,0	0,0	0,0
191	Nini-4A	1948,30	0,0	1,9	16,0	TR	0,0	0,0	10,1	0,0	1,0	39,9	27,1	0,8	3,0	0,0	0,0	0,0
192	Nini-4A	1948,60	0,0	2,5	17,0	0,0	0,0	0,0	3,9	0,0	2,9	0,0	69,0	0,0	2,8	TR	1,9	0,0
193	Nini-4A	1955,30	25,1	11,1	0,0	0,0	0,0	0,0	13,5	0,0	7,1	0,0	TR	0,0	0,0	43,2	0,0	0,0

Table 2 Mineralogy of the clay size fraction in the Nini 4 and 4A wells. The cap rock analyses are represented by the interval 1746.2–1766.46 m. From Humphrey & Lucas (2003).

XRD No.	Well		Depth(m)	Wt. %	Illite/smectite				Illite+Glauconite			Chlorite			Zeolite		Chert		Quartz		Calcite		Mg-Calcite		Pyrite	
				<16um	% A	% B	Order	%Illite	% A	% B	Crys	% A	% B	Crys	% A	% B	% A	% B	% A	% B	% A	% B	% A	% B	% A	% B
167	Nini-4		1746,20	50,7	65,0	33,0	RI	20-40	19,5	9,9	P	8,3	4,2	P	0,0	0,0	0,0	0,0	7,2	3,6	0,0	0,0	0,0	0,0	0,0	0,0
168	Nini-4		1746,41	56,0	51,6	28,9	RI	20-40	31,6	17,7	P	12,3	6,9	P	0,0	0,0	0,0	0,0	4,5	2,5	0,0	0,0	0,0	0,0	0,0	0,0
169	Nini-4		1749,09	78,8	49,6	39,1	RI	20-40	25,3	20,0	VP	8,4	6,7	P	7,6	6,0	0,0	0,0	9,0	7,1	0,0	0,0	0,0	0,0	0,0	0,0
170	Nini-4		1749,52	76,5	53,1	40,6	RI	20-40	22,5	17,2	VP	6,4	4,9	P	7,4	5,7	0,0	0,0	10,6	8,1	0,0	0,0	0,0	0,0	0,0	0,0
171	Nini-4		1757,20	59,9	60,3	36,1	RI	20-40	20,0	11,9	P	4,5	2,7	P	4,7	2,8	0,0	0,0	6,0	3,6	0,0	0,0	0,0	0,0	4,6	2,7
172	Nini-4		1762,20	58,3	58,1	33,9	RI	20-40	18,1	10,6	P	4,4	2,5	P	8,0	4,7	0,0	0,0	7,7	4,5	0,0	0,0	0,0	0,0	3,6	2,1
173	Nini-4		1766,41	34,5	37,6	13,0	RI	10-20	19,2	6,6	VP	0,0	0,0		0,0	0,0	34,1	11,8	4,9	1,7	0,0	0,0	0,0	0,0	4,3	1,5
174	Nini-4		1766,46	36,5	43,3	15,8	RI	10-20	14,4	5,3	VP	0,0	0,0		0,0	0,0	31,0	11,3	5,9	2,2	0,0	0,0	0,0	0,0	5,4	2,0
175	Nini-4		1771,04	14,5	33,3	4,8	RI/O	50-70	47,6	6,9	M	5,9	0,9	P	0,0	0,0	0,0	0,0	13,3	1,9	0,0	0,0	0,0	0,0	0,0	0,0
176	Nini-4		1774,03	13,4	30,8	4,1	RI/O	50-70	51,9	7,0	M	7,1	1,0	P	0,0	0,0	0,0	0,0	10,2	1,4	0,0	0,0	0,0	0,0	0,0	0,0
177	Nini-4		1777,04	11,1	10,9	1,2	O/LR	80-90	64,8	7,2	M	15,3	1,7	P	0,0	0,0	0,0	0,0	9,0	1,0	0,0	0,0	0,0	0,0	0,0	0,0
178	Nini-4		1780,04	13,2	10,1	1,3	O/LR	80-90	68,7	9,0	M	12,2	1,6	P	0,0	0,0	0,0	0,0	9,0	1,2	0,0	0,0	0,0	0,0	0,0	0,0
179	Nini-4		1783,12	15,9	8,5	1,4	O/LR	80-90	68,2	10,8	M	7,0	1,1	P	0,0	0,0	0,0	0,0	16,2	2,6	0,0	0,0	0,0	0,0	0,0	0,0
180	Nini-4		1783,81	32,5	88,9	28,9	RI	10-20	TR	TR	P	7,6	2,5	P	0,0	0,0	0,0	0,0	3,5	1,1	0,0	0,0	0,0	0,0	0,0	0,0
181	Nini-4		1788,56	32,2	20,7	6,7	RI	10-20	37,3	12,0	P	13,3	4,3	P	9,0	2,9	0,0	0,0	11,0	3,5	0,0	0,0	0,0	0,0	8,7	2,8
182	Nini-4		1788,76	17,4	35,1	6,1	RI	20-40	33,7	5,9	P	6,0	1,0	P	6,0	1,0	0,0	0,0	10,6	1,8	0,0	0,0	0,0	0,0	8,7	1,5
183	Nini-4		1852,11	13,1	7,3	1,0	O/LR	80-90	65,9	8,6	M	9,3	1,2	P	0,0	0,0	0,0	0,0	17,6	2,3	0,0	0,0	0,0	0,0	0,0	0,0
184	Nini-4		1856,10	17,8	37,0	6,6	RI/O	50-70	48,9	8,7	M	7,1	1,3	P	0,0	0,0	0,0	0,0	7,0	1,2	0,0	0,0	0,0	0,0	0,0	0,0
185	Nini-4A		1928,20	49,2	35,0	17,2	RI	20-40	14,6	7,2	VP	8,4	4,2	VP	0,0	0,0	30,3	14,9	6,9	3,4	0,0	0,0	0,0	0,0	4,8	2,4
186	Nini-4A		1932,50	13,5	27,2	3,7	RI/O	50-70	51,6	7,0	M	15,3	2,1	P/M	0,0	0,0	0,0	0,0	5,9	0,8	0,0	0,0	0,0	0,0	0,0	0,0
187	Nini-4A		1935,50	10,5	35,3	3,7	RI/O	50-70	45,8	4,8	M	14,8	1,6	P/M	0,0	0,0	0,0	0,0	4,1	0,4	0,0	0,0	0,0	0,0	0,0	0,0
188	Nini-4A		1938,50	14,2	20,0	2,8	RI/O	50-70	54,7	7,7	M	17,2	2,4	P	0,0	0,0	0,0	0,0	8,2	1,2	0,0	0,0	0,0	0,0	0,0	0,0
189	Nini-4A		1941,50	13,1	22,1	2,9	RI/O	50-70	53,3	7,0	M	18,8	2,5	M	0,0	0,0	0,0	0,0	5,9	0,8	0,0	0,0	0,0	0,0	0,0	0,0
190	Nini-4A		1944,50	12,9	23,9	3,1	RI/O	50-70	51,3	6,6	M	19,1	2,5	M	0,0	0,0	0,0	0,0	5,7	0,7	0,0	0,0	0,0	0,0	0,0	0,0
191	Nini-4A		1948,30	33,6	0,0	0,0			TR	TR	P	TR	TR	P	0,0	0,0	0,0	0,0	13,9	4,7	59,0	19,8	27,1	9,1	0,0	0,0
192	Nini-4A		1948,60	38,6	0,0	0,0			TR	TR	P	0,0	0,0		0,0	0,0	0,0	0,0	2,4	0,9	0,0	0,0	97,6	37,7	0,0	0,0
193	Nini-4A		1955,30	47,5	52,7	25,0	RI	20-40	23,4	11,1	P	0,0	0,0		0,0	0,0	0,0	0,0	4,0	1,9	0,0	0,0	0,0	0,0	19,9	9,4

In a regional context the clay minerals within the Paleogene to Neogene shales have been the topic of research for many years as documented by the clay mineralogy distribution map published by Nielsen et al. (2015) and with the most relevant maps shown here in Figs 16, 17 and 18.

In the stratigraphical period from Palaeocene to Oligocene i.e. including the Lista, Sele, Balder, Horda and Lark Formation smectite is the dominate mineral both in the bulk rock and in the clay size fraction (Nielsen et al. 2015). The source of the smectite was mainly weathered basaltic material introduced into the basin from volcanic activities due to the opening of the Atlantic Ocean (Figs 16–18). An additional illite/mica clay source was present that supplied material from the Norwegian basement and into the North Sea basin (Nielsen et al. 2015). Within this regional framework the mineralogical results documented from the Horda Formation in Nini-4/4A are in prefect agreement with the maps presented in Fig. 16.

3.4 Porosity and permeability of the cap rock

Porosity of the shales samples were measured by Geo, (2005), Nes et al. (2009) and Core Laboratories (2014). The porosities are generally high with values ranging between 15–25.8%. Nes et al. (2009) determined the porosity by weight loss measurements before and after drying at 109 ^{o}C and volume determined by Archimedes principle. Reported porosity were between 22.5 and 25.8% and grain densities were between 1.98–2.02 g/cm^3.

Nes et al. (2009) measured transient brine permeability of the Sele Formation sample from the Nini-5 well using a 3.5wt% NaCl solution and at confining pressure at 17.6 MPa. The permeability perpendicular to bedding was measured to 0.8 nD (sample 2 - 1686 m in the Nini-5 from the Sele Formation, Fig. 13). Permeability parallel to bedding was measured to be between 2–20 nD. Nes et al. (2009) argued that the variation could be due to microfractures i.e. damage of the sample. They did, however, contempt themselves and used the parallel to bedding permeability of 20 nD and reported the measurement as a valid value.

3.5 Rock mechanical data

Rock mechanical tests have been performed on all shale formations expect the Lark Formation (Geo 2005; Nes et al. 2009; Core Laboratories 2014) from where no core data from the Siri Canyon exist. The bulk of the tests were made on core material from the Sele and Lista Formations but also tests from the Horda Formation (the Sofie-1 well from 1873.25 m, Fig. 4) have been made (Geo, 2005). Due to the common mineralogical make-up of the shales deposited though the Palaeocene to Oligocene, however, the basic rock properties are very alike as seen with the analysis of plasticity of the shales and rock strength presented below. Most variation in the rock matrix appears rather to be related to the presence or absence of organic matter and/or radiolaria rich ooze.

Geo (2005) measured the unconfined compression strength (UCS) and also estimated it from the measured plasticity of the samples. Both the measured and estimated UCS were remarkedly similar given the range in stratigraphy. The estimated UCS ranged between 8.1–13.3 MPa with the lowest value for the Sele Formation and the highest value for Lista Formation and with the Horda Formation as having an intermediate value (10.1 MPa). Geo (2005) measured the UCS on fewer samples and the UCS obtained here ranged between 0.4–26.9 MPa pending on orientation of bedding.

Table 3 Results from triaxial testing. From Geo (2005).

Lab. no.	Formation	Height cm	Diameter cm	Density g/cm^3	Fluid cont. %	Orientation of bedding	$\sigma_{a,fail}$ MPa	$\sigma_{r,fail}$ MPa	c_u MPa
V1.50	Sele	7.634	3.807	2.28	10.3	≈ 50 ° to hor.	20.80	7.00	6.95
V3.90		7.702	3.820	2.28	9.6	0 ° to hor.	28.83	7.00	10.92
VX3.90		7.590	3.822	2.28	10.5	0 ° to hor.	19.46	3.50	7.98

Geo (2005) made three triaxial tests on the Sele Formation shale and measurements of acoustic properties were carried out at selected stress levels (Table 3). For all the tests, the sonic measurements are initiated in the last unloading phase and carried out during the undrained compression phase until failure. The results are presented below in Table 4.

Table 4 Acoustic measurements, Initial and final stress state. From Geo (2005).

Lab. no.	Formation	Stress state at start (σ_1, σ_3) MPa	Pore pressure (u_{top}, u_{bot}) MPa	Shear failure (σ_1, σ_3) MPa	No. of measurements
V1.50	Sele	(17, 10)	(0, 0)	(20.8, 7)	6
V3.90		(27, 27)	(2, 22)	(28.8, 7)	21
VX3.90		(27, 27)	(2, 22)	(19.5, 3.5)	70

On the basis of the acoustic determinations, the dynamic deformation parameters Poisson's ratio vdyn and modulus of Elasticity E1, dyn and E2, dyn (determined from vs1 and vs2, respectively) were determined (Table 5).

Table 5 Acoustic measurements, ranges of acoustic velocity. From Geo (2005).

Lab. no.	Formation	ν_{dyn}	$E_{1,dyn}$ MPa	$E_{2,dyn}$ MPa
V1.50	Sele	0.33-0.34	10620-10770	10240-10380
V3.90		0.12-0.15	14200-15100	13900-14940
VX3.90		0.13-0.17	13970-14960	13130-14680

GEO (2005) evaluated the plasticity of the shales (Table 6). According to the tests the shales have a medium plasticity index that compared to shales elsewhere in the North Sea rank them as moderate plastic shales.

Table 6 Plasticity of shales samples. From Geo (2005).

Well	Depth	Formation	Lab. no.	w_{nat} %	w_L %	w_P %	I_p %	Grain dens. g/cm^3
Na-2P	2074.8	Lista	A*	12.6	64.3	31.1	33.2	2.689
			B*		90.2	33.0	57.3	
			C*		92.7	32.7	60.0	2.663
	2074.9		D*	13.1	91.9	32.4	59.4	2.637
Vivi-1	1631.8	Sele	1	**	52.3	27.2	25.1	2.658
SCB-1X	2665.0	Sele	SCB-1X	**	50.3	24.7	25.7	2.758
Cecilie-2	2226.9	Sele (hot)	Cecilie-2	**	63.4	34.4	29.0	2.820
Sofie-1	1873.25	Horda	Sofie-1	**	76.1	37.7	38.4	2.744
Vivi-1	1659.75	Sele	Vivi-1	**	61.9	31.4	30.4	2.734

Table 2: Atterberg limit, plasticity index and grain density

* Sketch of location and orientation of specimens from Core 1 in Na-2P in Enclosure 11

** No water content – specimens were dried-out

Nes et al. (2009) reported the rock strength and noted that a significant heterogeneity exist with respect to the high gamma-ray "hot" zones in the Sele Formation. They also noted that the sample anisotropy is considerable. The UCS test results from the Sele Formation in the Nini-5 well (1686, 1703 m) range between 9.1–16.9 MPa and is thus within the estimated UCS range provided by GEO (2005) for a range of formations within the greater Nini area.

The results of triaxial testing made by Nes et al. (2009) are in their report presented in several tables (their table 3.5–3.9) and these are referred to these for test detail. In conclusion, they found that for the Nini-5 well that the intrinsic values for the strength are C_o=16.9 MPa and β=58.4°, while the weak plane values are C_{owp} = 7.0 MPa and β_{wp} = 51.9°. They conclude that the value of C_o was unexpectedly high.

Core Laboratories (2014) studied samples from the cap rock in the Solsort area (Solsort-2 wells) within the Tail End Graben that came from the depth interval between 2745.00–2767.50 m. The shales are slightly older than the seal rocks in the Nini West and also slightly deeper buried. Rock mechanics testing included triaxial compressive strength, acoustic velocity determinations and associated rock strength parameters obtained for hydraulic fracture design of the producing reservoir. Of importance for us is the rock mechanics analyses was designed to determine whether a fracture will be confined to the reservoir or not. From the shale interval in Solsort-2, two samples were submitted for triaxial compressive strength and acoustic velocity measurements (Table 7).

Table 7 Triaxial test results and fracture containment parameters. From Core Laboratories (2014).

Shale Interval		Triaxial Testing Results			Fracture Containment Parameters		
Sample Number	Depth (m)	Compressive Strength (psi)	Young's Modulus (10^6 psi)	Poisson's Ratio	Min Horizontal Stress (psi)	Fracture Gradient (psi/ft)	Fracture Toughness (psi-in$^{0.5}$)
A2-5	2745.23-2745.49	4431	0.35	0.27	7609	0.845	515
D4-5	2767.29-2767.50	4543	0.40	0.28	7706	0.849	552

Additional triaxial compressive strength with Mohr-Coulomb Failure analysis were made on eight samples. The triaxial compressive strength tests are commonly used to simulate the in-situ stress conditions of the reservoirs and provide compressive strength and static values of elastic constants: Young's modulus and Poisson's ratio. Young's modulus is the slope of a line when axial stress is plotted against axial strain. An important property of linear-elastic material is the ability to expand in a lateral direction when the load is applied on the material in a vertical direction. This ability to expand laterally is expressed by Poisson's ratio, which is defined by the ratio of lateral expansion to vertical contraction. Poisson's ratio is a critical parameter in determining formation stress and consequently influences fracture height and width. The results from the triaxial testing, which includes Young's modulus and Poisson's ratio, is summarized in Table 8.

Table 8 Triaxial compression strength, Youngs Modulus and Poisson ratio. From Core Laboratories (2014).

Shale Interval Triaxial Compressive Strength

Sample Number	Depth (m)	Confining Pressure (psi)	Compressive Strength (psi)	Young's Modulus (10^6 psi)	Poisson's Ratio
A2-3	2745.23-2745.49	200	1184	0.29	0.27
A2-2		910	3186	0.32	0.28
A2-4		1820	4529	0.36	0.27
A2-1		2730	6800	0.41	0.28
D4-1	2767.29-2767.50	200	1550	0.32	0.29
D4-3		910	3251	0.34	0.29
D4-4		1820	4801	0.42	0.28
D4-2		2730	6917	0.48	0.27

3.6 Well leak of pressure and tests in Nini wells

Abundant data on the seal rock strength, fracture gradient and seal capacity exist for the Nini Field Complex collected during drilling of the wells and from data collected as part of testing of the connections. These data include leak of pressures and leak of tests and pressure obtained from MDT testing.

For this report these data have been complied for the Nini-1 to 5 wells and presented in Fig. 19 and the following description has been added from information obtained from INEOS. In Fig. 19 the envelope of minimum shale fracture gradients (minimum stress) from TD and up to about 1100 m is represented by the dashed grey line in Fig. 19. The shale fracture gradient (FGs) were calculated with an effective stress ratio (minimum effective stress to maximum/vertical effective stress) of 0.72. The threshold of minimum sand "FG" on Fig. 19 is indicated by the dashed orange line. The location of this envelope was determined by recalculating the low-end FG with a new effective stress ratio of 0.55, which is as low as have seen anyone use for an effective stress ratio in a sand.

At current the analysis of the data presented in Fig. 19 is not completed and therefor the information than can be obtained from these has not be used to the full extend. The analyse will see also see if the fracture propagation pressure can be established form the leak of tests since we note that similar type of data has been successively applied elsewhere when CO_2 storage containment capacity have been evaluated (c.f. Bohloli et al. 2014).

4.0 RISK ASSESSMENT OF SEAL CAPACITY AT NINI WEST

Assessing the Cap rock capacity and risking is a multidisciplinary exercise and depends on several aspects. We here follow the methodology outlined by Bruno et al. (2014) that has developed a Quantitative Risk & Decision Analysis Tool (QRDAT) methodology for caprock integrity evaluation. The methodology uses an established set of parameters (risk factors) that influence the likelihood of caprock failure. The method has established order of magnitude value ranges for each parameter, which, when applied to geologic and operational settings, enable quantification of risk, and offer a means by which to compare potential and active storage sites.

The Bruno et al. (2014) model consider three primary leakage mechanisms. These are tensile fracturing of the caprock, fault activation, and well damage. The set of risk factors can be divided into three main groups:

1. Mechanical state of the storage system, which includes stresses, pressures, and faults.
2. Caprock and storage zone system, including reservoir and caprock geometry and properties; and
3. Operations, which include the status of the wells and injection practices.

In Table 9 we have presented the results for the risk analysis and below we evaluate the Risk Factors in the Quantitative Risk & Decision Analysis Tool (QRDAT) system and its applicability to Nini West proposed Storage Site:

Table 9 Preliminary risk matrix for the Nini West seal complex. Risk factors are after Bruno et al. (2014). Green colour indicate that the risk factor has been evaluated with a reasonable confidence. Blue colour that the risk factor is only provisionally assessed here. Note that not all risk factors have currently been evaluated.

Risk factor	Risk factor value ranges		
	High risk	**Moderate risk**	**Low risk**
Lateral extension of the storage zone/formation depth	< 25	25–100	> 100
Storage zone thickness/storage zone depth	> 0.5	0.1–0.5	< 0.1
Stress regime	Compressional	Transform	Extensional
Caprock strength	Weak	Moderate	Strong
Caprock thickness	≤ 3 m	3–30 m	≥ 30 m
Fault boundaries	Multiple	One	≥ 30 m
Natural seismicity	High	Moderate	Low
Number of caprocks	No	One	Multiple
Maximum formation pressure/formation depth	≥ 0.75	0.625–0.75	≤ 0.625
Desired maximum formation pressure/discovery pressure	≥ 1.5	1.25–1.5	≤ 1.25
Well density	> 15 km^2	5–15 km^2	< 5 km^2
Number of uncased wells/total number of wells	> 0.6	0.2–0.6	< 0.2
Temperature difference between the injected CO_2 and the ambient storage zone temperature	≥ 60°C	30–60 °C	≤ 30 °C
Caprock heterogeneity	Significant	Moderate	Strong
Caprock permeability	> $10^{-15} m^2$	10^{-18} – 10^{-15} m^2	< 10^{-18} m^2
Caprock lateral extend/storage zone thickness	< 25	25–100	> 100
Caprock dip	≥ 8°	2°–8°	≤ 2°
Minimum horizontal stress/vertical stress (stress ratio)	< 0.55	0.55–0.65	> 0.65

4.1. Mechanical State Factors

4.1.1. Desired maximum formation pressure/effective minimum horizontal stress

The higher this ratio, the higher the risk for caprock failure. This number is a measure on how close the pressure in the formation is to the failure pressure, as fracturing occurs when the minimum horizontal stress is exceeded by the pressure in the reservoir. In the Nini West the desired formation pressure during CO_2

storage is expected to be slightly above 200 bara and the maximum injecting pressure is expected to be 350 bara (Project Greensand Phase 1 - Feasibility Report 2020). Estimation of the effective minimum horizontal stress can be evaluated from leak of test and leak off pressure established from the drilling process (c.f. Fig. 19). From this the leak of pressures equivalent of a mud weight of 1.8 sg are observed corresponding to 305 bara. At this time the leak of pressure model has not been evaluated by the lead author and the pressure profile for the pilot injection phase in the Nini West has not been established and hence the ratio between the desired maximum formation pressure to effective minimum horizontal stress cannot be evaluated.

4.1.2. Desired maximum formation pressure/discovery pressure

The discovery pressure at the Nini West field was 189 bara and at current the reservoir pressure is at 209 bara due to water injection (Project Greensand Phase 1 - Feasibility Report 2020). The current scenario for CO_2 storage is to slightly exceed the initial pressure i.e. to be near the current pressure in the reservoir at storage situation and thus that the proven cap rock capacity will only be slightly exceeded. Therefore, this ratio is expected to be < 1.25 (209/189 bar/bar) in the storage mode reflecting a low pressure increase in the caprock-storage zone system. The low pressure increases lower the potential for tensile and shear failure in the caprock and thus poses low risks for CO_2 containment failure. The maximum desired formation pressure during injection mode is 350 bara. The resulting pressure profile in the reservoir-cap rock system has not yet been made available for analysis (see 4.1.1). Until the pressure profile for the pilot injection phase in the Nini West is established the ratio between the desired maximum formation pressure to discovery pressure cannot be evaluated.

4.1.3. Maximum formation pressure/formation depth

Risk for caprock failure depends on formation pressure and as this increase so do the risk. The pressure, however, needs be normalized to the formation depth to consider the fact that high pressures are less influential with increasing depth due to countervailing pressure increases from increasing overburden load. In the Nini West initial pressure was 189 bar (2740 psi) and current pressure 209 bar (3030 psi). The ratio for Nini West with a reservoir depth of 1734 TVDMS (5680 ft) is 0.48 (3030/5680 psi/ft). This ratio is low and thus signals a low risk for integrity loss. However, until the pressure profile for the pilot injection phase in the Nini West is established the ratio between the maximum formation pressure to formation depth cannot be evaluated.

4.1.4. Stress regime

Simple stabilization relations imply that a compressional stress regime will have the highest risk for reactivation during CO_2 injection, as CO_2 pressure increase will have a destabilizing effect on thrust faults, whereas it has stabilizing effect on normal faults. This only refers to the normal stresses induced by pressure increase. It does not refer to possible direct migration of fluid into the fault zone, which can destabilize either type of fault by reducing the normal effective stress acting to keep the fault from slipping. The Nini West field is situated in an area with low tectonic stress. The regional stress field is influenced by the North Atlantic Ridge Push and thus an overall compressional regime can be inferred. This push is translated into transform stresses in the North Sea. For risking we thus infer a medium level. This evaluation is tentative and awaits further interpretation of data to complete the analysis. Well break-out data would be an important source of information, however, we doubt that the reactive nature of the shales would allow such data to be collected. The Nini West fields stress field may also be influenced by the presence of salt diapir in the subsurface. Stress in the subsurface was, however, expected to have been released during the fluidization vents that affected the reservoirs.

4.1.5. Stress ratio

The stress ratio is defined as the ratio of minimum effective stress ($\sigma 3$) to maximum/vertical effective stress ($\sigma 1$). Modelling studies for extensional stress regimes have shown that lower stress ratios lead to larger absolute fault slip magnitudes. In general, stress ratios are on the order of 0.5 – 0.7. Lower stress ratios lead to greater fault reactivation risks due to enhanced arching of the resulting normal stress. This causes a larger normal than shear stress ratio and so a greater chance of fault activation. In Nini West due to slight compression to transform stress field we tentatively infer a medium to high ratio are thus a medium to low risk. As with section 4.1.4. this aspect will be further evaluated.

4.1.6. Fault boundaries

Faults can be activated by supercritical CO_2 encroachment and fault reactivation at the caprock-reservoir interface increase this location's sensitivity to integrity loss (Bruno et al. 2014). In the Project Greensand Phase 1 - Feasibility Report (2020) it is shown that the mapped faults propagate for relatively short lateral and vertical distances. For this report it is stated that the apparent lack of pressure communication between the three Nini reservoir units is considered also as evidence that the existing faults are not transmissible. In the vertical direction, all faults appear to heal at or below the lower Oligocene level, with no faults propagating anywhere close to known permeable units of the overburden (Nolde Sand Formation). It is therefore concluded that the existing faults do not represent a risk of leakage.

4.1.7. Natural seismicity

The Nini West Field is situated in an area of low natural seismic activity, away from active fault zones or subsiding areas. Low natural seismicity clearly poses a low risk for caprock integrity loss. In contrast in regions with strong natural seismicity, the presence of pre-existing faults and fracture networks can be expected to be reactivated, which offer potential conduits for fluid migration, and generally reduce caprock integrity. We thus infer that the structural position of the Siri Canyon possesses a low risk for natural seismic events to causes any integrity losses.

4.2. Caprock-Storage Zone System Factors

4.2.1. Storage zone lateral extent/depth and caprock lateral extent/thickness

The seal complex in the Nini West field extend regionally in the North Sea and even outcrop onshore Denmark. This assures the lateral continues of the seal. According to Bruno et al. (2014) we have normalised the caprock thickness to extent and there is only a small the chance that CO_2 will migrate upwards as reflected is the high value.

Assessment of the Storage zone lateral extent awaits analysis of the 3D model.

4.2.2. Storage zone thickness/ depth

High values for this ratio correspond to a relatively thick reservoir at relatively shallow depth, indicating relatively large volumes of CO_2 stored relatively close to the surface. This combination has a major implication if failure in the caprock occurs: the release of a large amount of CO_2 without far to migrate upwards to reach the surface. Thus, high ratio values here correspond to high risk. For the Nini West storage site a relative thin storage zone thickness compared to depth is expected. At depths of 1740 TVDMS the ratio for the reservoir storage unit is expected to be within 0.1–0.5. This final evaluation of this ratio will be made from analysis of the 3D model.

4.2.3. Caprock strength

A stronger caprock has a lower risk for caprock integrity loss, due to a lower risk for both tensile fracturing and the onset of new faults in the caprock. A fracture develops only when the compressive strength in a rock is overcome, so the higher the unconfined compressive strength the lower the risk for the development of fracture networks. The Palaeocene shales in the Nini area range with a UCS of 8–16 MPa and is thus classified as a weak to moderate strong caprock. In the risk assessment made here, we tentatively assign the risk as moderate and awaits further classification and assessment of the rock strength in the Nini West area. We expect to apply a wire-line based approach to cap rock strength analysis based on analysis of the dynamic properties. This also since the cap rock has a considerable thickness with over 300 m for the primary seal and 500 m for the secondary seal. For these seals cores only exist for a limited part and no fresh material is available for new tests. Thus, complete formation analysis of the seal strength will have to rely on a wire-line approach.

We note that for this special smectite rick shales with a medium plasticity the presence of brine along facture planes might change the strength of the formation considerably. Plastic deformation may thus be important and self-healing of any fractures network maybe a more pronounced for this shale.

4.2.4. Caprock permeability

Relatively permeable caprocks may lead to loss of CO_2 containment, simply because CO_2 can migrate through them under the influence of strong buoyancy forces. This can occur for caprocks with permeabilities as low as $k > 10^{-18}$ m^2. In the Nini East brine permeabilities in the nD (10^{-21} m^2) range has been measured indicating that integrity loss due to caprock permeabilities is expected to be low. As part of the Project Greensand more characterisation of the permeabilities will be made including measurements of air-permeabilities and permeabilities to CO_2 will be esteemed from MICP data on a broad range of depths from the primary seal. Also, the specific surface area will be measured allowing the permeability to be modelled directly from this.

4.2.5. Caprock dip

Caprock dip mainly influences the migration of CO_2 within the reservoir. Due to high buoyancy of the CO_2, the supercritical fluid will tend to move upward in the reservoir until structurally trapped. The greater the caprock dip, the further the CO_2 migrates upwards, with the risk of reaching a spill point or discontinuity in the caprock also increasing. Also dipping caprock-storage zone systems lead to preferred CO_2 migration in the up-dip direction. The greater the dip, and its extent, the more quickly, and further, the CO_2 may migrate laterally. The Nini West trap is a combination of structural and stratigraphic trap along the western flank of the Nini Salt Dome (Project Greensand Phase 1 - Feasibility Report, 2020). The structural dip is not addressed specifically but is assumed here to be up to 8^o and thus it may pose a medium risk. The final evaluation of this is, however, to be made from the 3D model and thus this risk aspect is not evaluated here.

4.2.6. Caprock thickness

The seal at the Nini West field is composed by the primary 340 m thick seal unit composed by the Horda Formation and the lower to mid Lark Formation and the c. 550 m thick secondary seal composed by the mid to upper Lark Formation. The combined seal complex is thus c. 900 m thick. According to Bruno et al. (2014) such thick caprock lower the risk for integrity loss, simply because fracture networks and faults can develop further into the caprock without fully transgressing it. For example, at the operating In Salah CO_2 storage site a fracture network reaches 100–200 m into the caprock (Verdun et al. 2013), but since the caprock package is up to 950 m thick, this has no effect on the security of storage (Bruno et al. 2014). Therefor we consider the caprock thickness to pose a very low risk for the Nini West.

4.2.7. Caprock heterogeneity

Caprock heterogeneity increases the risk for integrity and containment loss for various reasons. First, in case of lateral heterogeneity (e.g. in turbidite settings), CO_2 may reach discontinuities in the caprock, which may allow upward migration. In very heterogeneous caprocks, connected fluid pathways to higher strata may be present. Second, heterogeneity of lithology within the caprock may lead to stress concentrations, rendering these interfaces prone to tensile and shear failure. In the Nini West the main lithology is pelagic mud deposition interrupted by mud to more coarse-grained turbidite systems. The bottom environment was periodically anoxic providing strong anisotropy and periodically allowed radiolarian to accumulate. For the seal complex at Nini West the similarity of the succession in term of the mineralogy and hemipelagic nature of the deposition is remarkably similar. The frequency of sand and silt streaks report is low and evaluated to pose low risk of being interconnected. The caprock heterogeneity is thus evaluated as “strong” i.e. on the lowest heterogeneity level according to Bruno et al. (2014) classification, which rank the Nini West seal with a low risk for integrity loss.

4.2.8. Number of sealing strata

The number of individual sealing strata within the general caprock package influences the integrity of the system simply by forming a baffled system of multiple storage locations with multiple caprocks which act as buffers if the primary seal below them fails. However, the existence of multiple caprocks is by itself not a guarantee for CO_2 containment, however, in general the risk for integrity loss decreases with an increasing number of caprocks above the primary intended seal. In the Nini West the Seal is composed by two thick main seals, the primary and the secondary, and each of these main seals are composed by several formations and units. In summary, the Nini West Seal Complex thus have multiple seal strata and for this reason little risk for integrity loss is expected based on this parameter.

4.3. Operations Risk Factors

4.3.1. Well density

The number of wells already drilled through the caprock clearly increases the risk of CO_2 migration. The greater the number of wells that fully penetrating the caprock and into the storage zone, the greater the number of potential leakage pathways thus present. In the Project Greensand Phase 1 - Feasibility Report (2020) three legacy wells exist including the exploration well Nini 4 and its side-track 4A, the produced Na-03A and the injector well Na-05. The legacy well count is thus four in the Nini West. The relevant area for this number to normalised to be defined later but is about 1 km^2 and therefor it is expected that the ratio will be less than 5 legacy well pr. km^2 and therefore only pose a low risk for integrity loss according to the scheme of Bruno et al. (2014).

4.3.2. Number of uncased wells/total number of wells

Best CO_2 practices currently dictate that new well casings are to be designed to stay intact for timescales on the order of thousands of years. The biggest risk overall for safe CO_2 storage is posed by old abandoned wells, residing mainly in depleted hydrocarbon reservoirs, which were not designed for secure storage for timescales of this magnitude. In the Project Greensand Phase 1 - Feasibility Report (2020) these conditions and requirements are also addressed; however, the number of cased wells was not reported and thus this ratio cannot be evaluated.

4.3.3. Temperature difference between injected CO_2 and storage zone

The initial reservoir temperature in the Nini West field was 60^{o}C but is now lowered due to water injection. At current the temperature of the delivered CO_2 is not fixed. It can be expected to be low (10 ^{o}C) but pending on conduction on ship we assume that this could be delivered also higher and a current this temperature difference cannot be evaluated. We note, however, that the temperature difference is not expected to be higher than 50^{o}C. For this temperature difference a medium to low thermal difference between the injected CO_2 stream and reservoir will exist which will pose a medium to low risk (Bruno et al. 2014).

5.0 BENCHMARKING OF THE NINI WEST SEAL CAPACITY

We have applied the risk assessment and evaluated the Nini West Field in the same manner as Bruno et al. (2014) evaluated five other CO_2 injection and potential injection sites. The first three sites evaluated by Bruno et al. (2014) are potential CO_2 sites under consideration, including the Kevin Dome site, the Louden site, and the Wilmington Graben. Two others are actual large-scale CO_2 injection sites, including Sleipner in the North Sea and In Salah in North Africa.

The evaluation of the Nini West presented here is not complete yet and therefor a direct comparison to the total risk score presented by Bruno et al. (2014) for the evaluated sites cannot be made at this stage. For the Nini West, none of the completed evaluated parameters are, however, in the high risk category which make the Nini West likely to receive an overall low risk score.

6.0 CONCLUSIONS

The Siri Canyon is characterised by overall low natural seismicity. The latest tectonic event that affected the North Sea area was the opening of the North Atlantic and as consequence ridge push forcers still affects Northern Europe. The primary seal to the Nini West Field is in the Nini-4 well 340 m thick and composed of shales that belong to the Eocene to Miocene Horda Formation and the lower to mid Lark Formation. The Horda Formation is characterised by greenish grey to greyish green fissile mudstone. Subordinate limestone benches and thin layers of black mudstones occur at some levels in the formation. The lower Lark Formation is dominated by dark, greenish grey, non-fissile mudstones with subordinate intervals of brownish grey mudstones. The secondary seal is in the Nini-4 well 550 m thick that belong to the mid to upper Lark Formation. This shale is composed by pale to dark brownish grey mudstones with subordinate intervals of greenish grey mudstones. The combined seal sequence is thus almost 900 m thick in the Nini West area. The above lying strata i.e. the remaining c. 800 m of strata that belongs to the Nolde Sand and the Nordland Group is considered overburden.

During formation of the primary and secondary seal, smectite was the dominate clay mineral and due to the common mineralogical make-up of the shales the basic rock properties are very alike between the different shale formations as seen from analysis of the plasticity of the shales and the rock strength tests. Most of the variation appear to be related to the presence or absence of organic matter and/or radiolaria rich material that may or may not be present in all formations.

Measured porosities range between 15–25.8% for the lower Hordaland Group and measured transient brine permeability of the Sele Formation range between 1 and 20 nD pending on being orientation.

Rock mechanical tests have been performed on all shale formations expect the Lark Formation from where no core data from the Siri Canyon exist. The bulk of the tests were made on core material from the Sele and Lista Formations but also tests from the Horda Formation have been made. Unconfined compression strength (UCS) (measured and estimated) range between 8.1–13.3 MPa with the lowest value for the Sele Formation and the highest value for Lista Formation and with the Horda Formation as having an intermediate value (10.1 MPa).

We present a risk analysis for the seal capacity for the Nini West field seal complex following the risk factors presented by Bruno et al. (2014). The risk factors include 18 different parameters of which the current state of knowledge allows 12 to be evaluated here either with a reasonable certainty or provisionally pending on more data and analysis. The evaluation show that none of the evaluated parameters falls within the high-risk category of Bruno et al. (2014) and that most of the evaluated risk factors fall within the low to medium risk group. Most of the risk parameters that has been assigned a medium risk need, however, additional analysis and characterisation before final evaluation can be made. Compared to other seal complexes evaluated according to the Bruno et al. (2014) risk scheme, then the caprock capacity of the Nini West Field currently have a relative low risk score although not all risk factors have currently been evaluated.

ACKNOWLEDGMENT

The Danish Energy Technology Development and Demonstration Program (EUDP) is greatly acknowledged for its funding of the "Project Greensand". The Project Greensand is carried out by INEOS, Maersk Drilling and Wintershall DEA and the lead author thanks the team for valuable comments and suggestions that improved the content of this report.

7.0 REFERENCES

Arfai, J., Franke, D., Lutz, R., Reinhardt, L., Kley, J. & Gaedicke, C., 2018: Rapid Quaternary subsidence in the northwestern German North Sea. Scientific Reports 8, Article number: 11524. https://doi.org/10.1038/s41598-018-29638-6

Project Greensand Phase 1 - Feasibility Report (2020). Report prepared by Project Greensand.

Ask, M.V.S., Müller, B. & Stephansson, O. 1996: *In situ* stress determination from breakout analysis in the Tornquist Fan, Denmark. Terra Nova 8, 575 – 584.

Bohloli, B., Skurtveit, E., Grande, L., Titlestad, G.O., Børresen, M.H., Johnsen, Ø. & Braathen A. 2014: Evaluation of reservoir and cap-rock integrity for the Longyearbyen CO_2 storage pilot based on laboratory experiments and injection tests. Norwegian Journal of Geology, Vol 94, pp. 171–187. Trondheim 2014, ISSN 029-196X.

Bruno, M.S., Lao, K., Diessl, J., Childers, B., Xiang, J., White, N. & van der Veer, E. 2014: Development of improved caprock integrity analysis and risk assessment techniques. Energy Procedia 63, 4708–4744.

Damtoft, K., Andersen, C. & Thomsen, E. 1987: Prospectivity and hydrocarbon plays of the Danish Central Trough. In: Brooks, J. & Glennie, K.W. (eds), Petroleum geology of North-West Europe, 403–417. London, Graham & Trotman.

DONG, 2003: Core sedimentology. Licence 4/95 Well Nini-4. DONG rep 16088, 24 pp.

GEO, 2005: Nini overburden stability problems. GEO project no 26862. Report 1, 1–23.

Gregersen, S., Linholm, C., Korja, A., Lund, B., Uski, M., Oinonen, K., Voss, P.H. & Keiding, M., in press. Seismicity and sources of stress in Fennoscandia.

Hamberg, L., Dam, G., Wilhelmson, C. & Ottesen, T. 2005: Paleocene deep-marine sandstone plays in the Siri Canyon, offshore Denmark—southern Norway. In: Dore´, A.G., Vining, B.A. (Eds.), Petroleum Geology: North-West Europe and Global Perspectives—Proceedings of the 6th Petroleum Geology Conference, Petroleum Geology Conferences Ltd. Geological Society, London, pp. 1185–1198.

Humphrey, N. & Lucas, P.M. 2003: Wells Nini-4 and Nini-4A, Offshore Denmark, Petrographic Study of lower Tertiary Sediments. Report No. 8658/Id. Robertson Research International, 49 p with three appendices.

Heidbach, O., Rajabi, M., Cui, X., Fuchs, K., Müller, B., Reinecker, J., Reiter, K., Tingay, M., Wenzel, F., Xie, F., Ziegler, M.O., Zoback, M.-L. & Zoback, M.D. 2018: The World Stress Map database release 2016: Crustal stress pattern across scales. Tectonophysics, 744, 484–498. http://doi.org/10.1016/j.tecto.2018.07.007

Jensen, T.D., Voss, P.H., Larsen, T.B. & Gregersen, S. 2013: Seismic activity in Denmark: detection level and recent felt earthquakes. Geological Survey of Denmark and Greenland Bulletin 28, 41–44.

Kazerouni, A.M., Friis, H., Svendsen, J.B. & Nielsen, O.B. 2013: The effect of burial on clay mineral diagenesis and quartz cementation in mudstones examples from the Siri Canyon, Danish North Sea. in A.M. Kazerouni (ed.), Sandstone: Geochemistry, Uses and Environmental Impact. Nova Science Publishers, pp. 271-295.

Millennium Atlas Chapter 14 (2001). In: Evans, D., Graham, C., Armour, A. & Bathurst, P. (editors and compilers), The Millennium Atlas: Petroleum Geology of the Central and Northern North Sea. Geological Society of London, Bath, London.

Millennium Atlas Chapter 16 (2001). Nordland Group. Millennium Atlas Chapter 16 In: Evans, D., Graham, C., Armour, A. & Bathurst, P. (editors and compilers), The Millennium Atlas: Petroleum Geology of the Central and Northern North Sea. Geological Society of London, Bath, London.

Nes, O.-M., Sønstebø, E.F. & Bøe, R. 2009: Geomechanical and petrophysical testing of Sele Shale. SINTEF report no 33.5582.00/01/09, 139 p

Nielsen, L.H. 2003: Late Triassic-Jurassic development of the Danish Basin and Fennoscandian Border Zone, Southern Scandinavia. In: Ineson, J. and Surlyk, F. (eds.): The Jurassic of Denmark and Greenland. Geological Survey of Denmark and Greenland Bulletin 1, 459–526.

Nielsen, O. B., Rasmussen, E.R. & Thyberg, B.I. 2015: Distribution of clay minerals in the northern North Sea basin during the Paleogene and Neogene: A result of source-area geology and sorting processes. Journal of Sedimentary Research, 2015, 85, 562–581. DOI: http://dx.doi.org/10.2110/jsr.2015.40

Ohm, S.E., Karlsen, D.A., Roberts, A., Johannesen, E. & Høiland, O. 2006: The Paleocene sandy Siri Fairway: An efficient “pipeline” draining the prolific Central Graben? Journal Petroleum Geology 29, 53–82.

Verdon, J.P., Kendall, J.M., Stork, A.L., Chadwick, R.A., White, D.J. & Bissell. R.C. 2013: Comparison of geomechanical deformation induced by megatonnescale CO_2 storage at Sleipner, Weyburn, and In Salah. Proceedings of the National Academy of Sciences 2013, 110, E2762-E2771.

Petersen, H.I., Hertle, M., Juhasz, A. & Krabbe, H. 2016: Oil family typing, biodegradation and source rock affinity of liquid petroleum in the Danish North Sea. Journal of Petroleum Geology 39, 247–268. https://doi.org/10.1111/jpg.12645

Schiøler, P., Andsbjerg, J., Clausen, O.R., Dam, G., Dybkjær, K., Hamberg, L., Heilmann-Clausen, C., Johannesen, E.P., Kristensen, L.E., Prince, I., & Rasmussen, J.A. 2007: Lithostratigraphy of the Palaeogene–Lower Neogene succession of the Danish North Sea. Geological Survey of Denmark and Greenland Bulletin 12, 77 pp.

Schovsbo, N.H., Ponsaing, L., Mathiesen, A., Bojesen-Koefoed, J.A., Kristensen, L., Dybkjær, K., Johannessen, P., Jakobsen, F. & Britze, P. 2020: Regional hydrocarbon potential and thermal reconstruction of the Lower Jurassic to lowermost Cretaceous source rocks in the Danish Central Graben. Bulletin of the Geological Society of Denmark 68, 195–230.

Stokkendal, J., Friis, H., Svendsen, J.B., Poulsen, M.L.K. & Hamberg, L., 2009: Predictive permeability variations in a Hermod sand reservoir, Stine Segments, Siri Field, Danish North Sea. Marine and Petroleum Geology 26, 397–415.

Svendsen, J., Schovsbo, N. & Friis, H. 2011: Biodegradation of Oil in a Tertiary mass flow system - Implication for reservoir quality and performance in the Nini East Field, Danish North Sea. Tertiary fan reservoirs of the North Sea, Conference abstracts, p. 40.

Svendsen, J.B., Hansen, H.J., Stærmose, T. & Engkilde, M.K. 2010: Sand remobilization and injection above an active salt diapir: the Tyr sand of the Nini Field, Eastern North Sea. Basin Research 22, 548–561. https://doi.org/10.1111/j.1365-2117.2010.00480.x

Voss, P., Jensen, T.D. & Larsen, T.B. 2005: Earthquake Hazard in Denmark. GEUS Rapport 2015/24, 1–53.

Weibel, R., Friis, H., Kazerouni, A.M., Svendsen, J.B., Stokkendal, J. & Poulsen, M.L.K. 2010: Development of early diagenetic silica and quartz morphologies — Examples from the Siri Canyon, Danish North Sea. Sedimentary Geology 228, 151–170.

FIGURE CAPTIONS

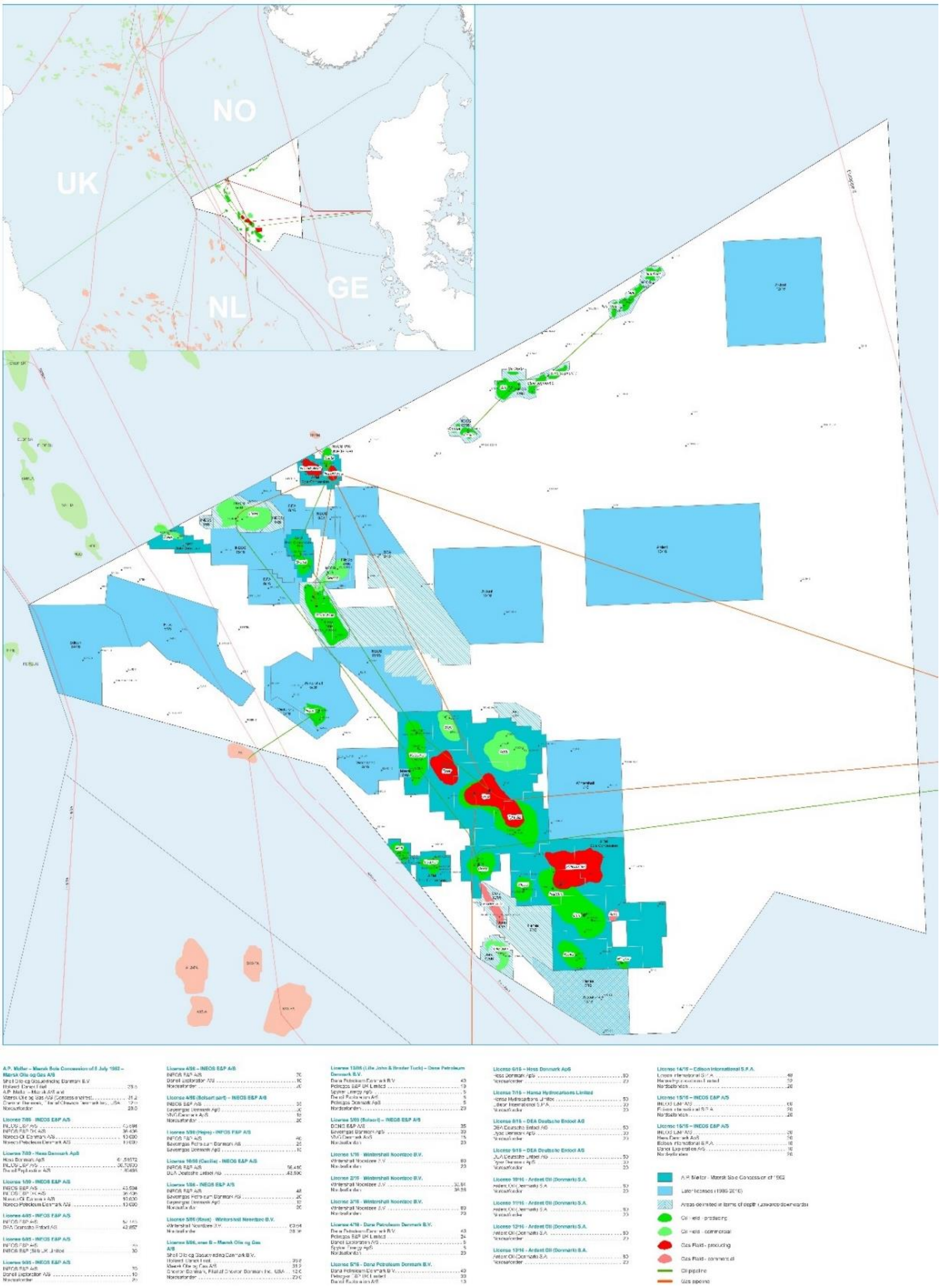

Figure 1 Danish oil and Gas fields. From the Danish Energy Authorities (DEA).

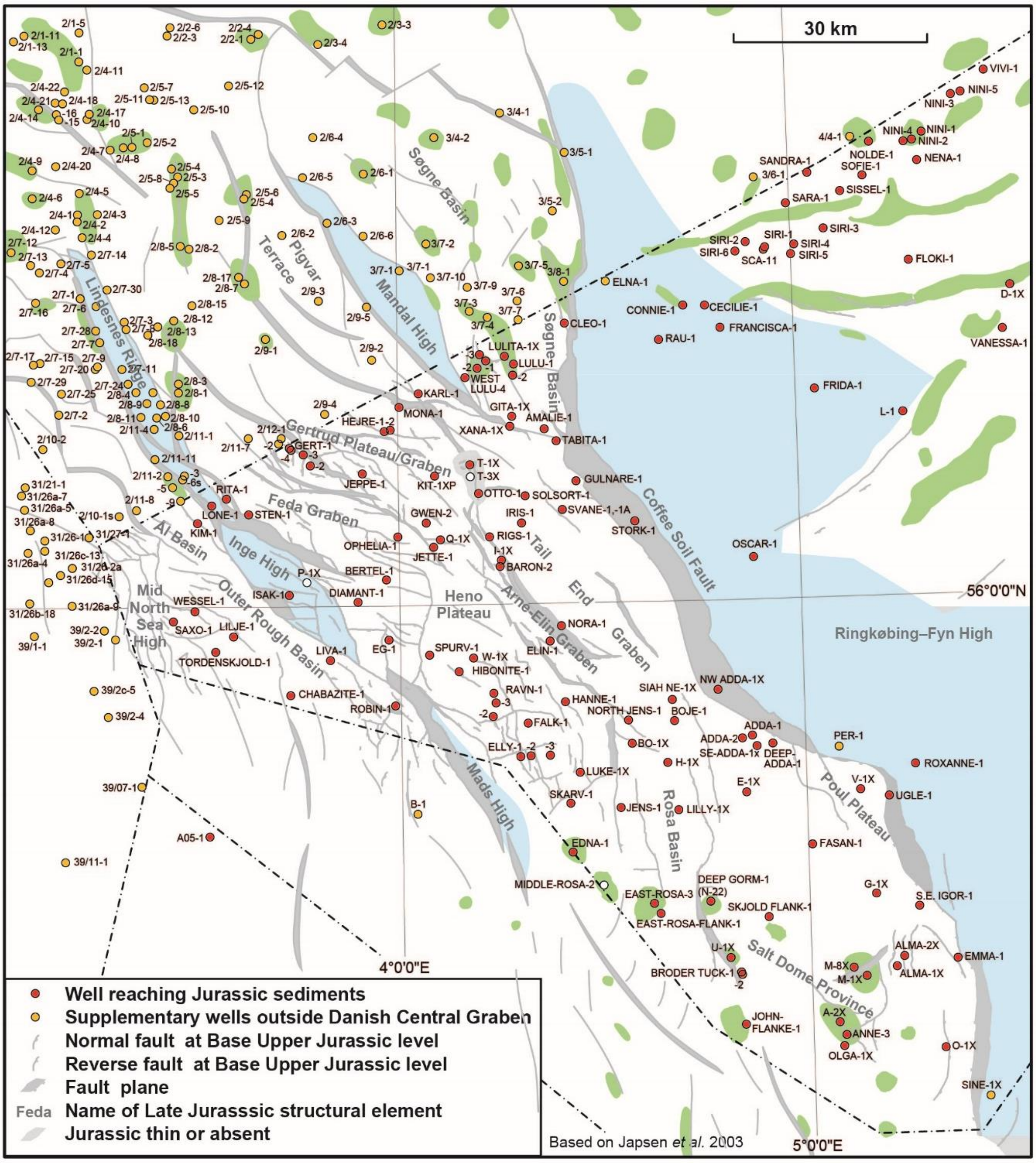

Figure 2 Well locations. Modified from Schovsbo et al. (2020).

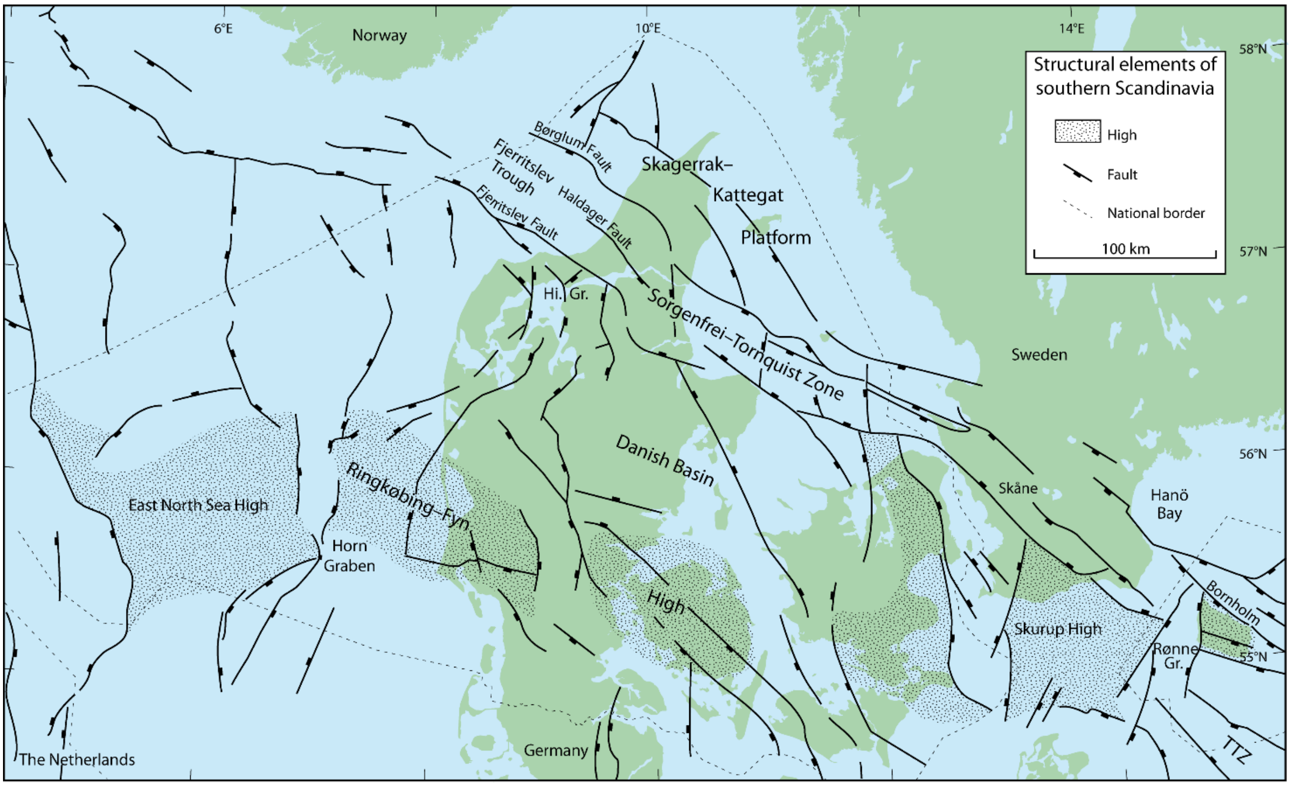

Figure 3 Structural map of Denmark. From Nielsen (2003).

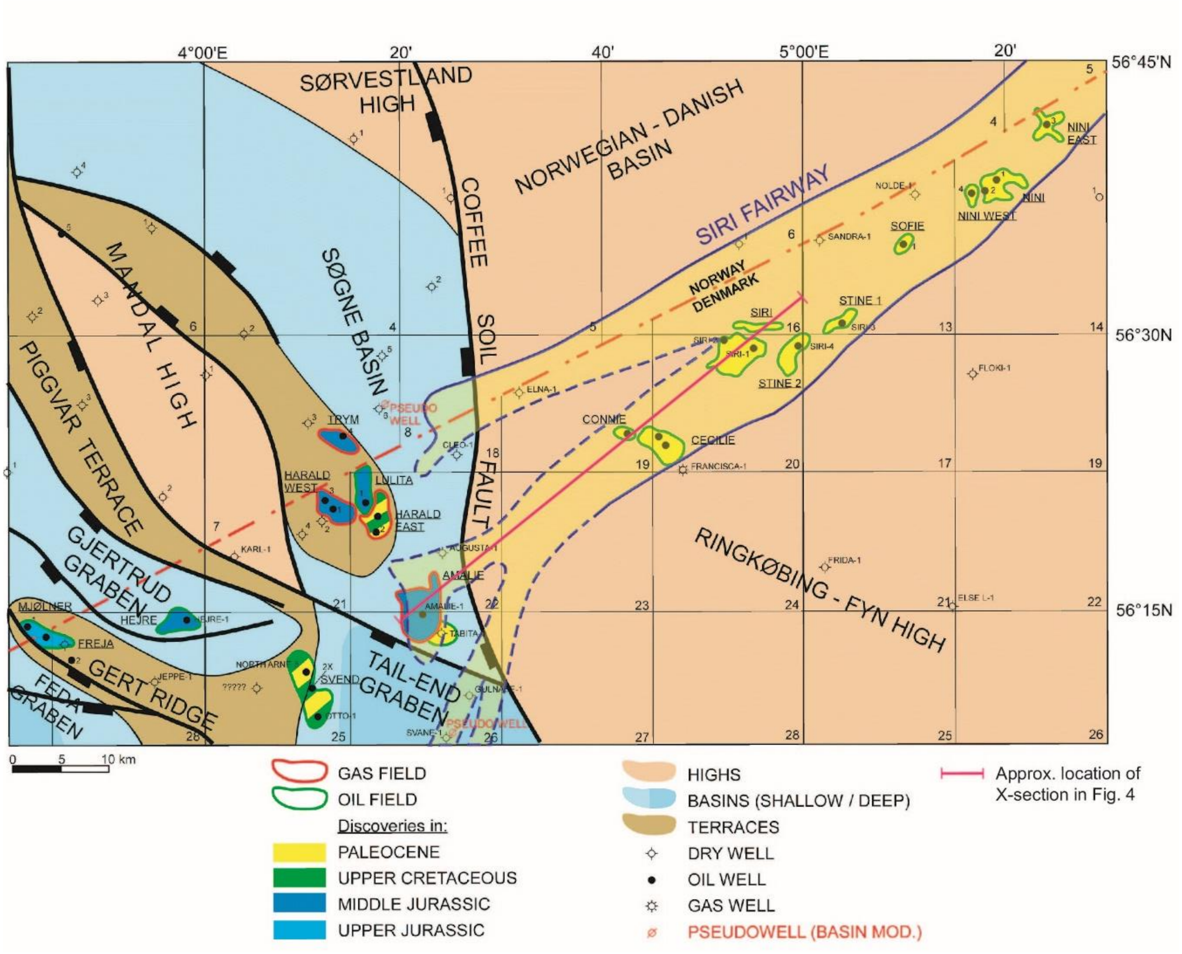

Figure 4 Siri Canyon with fields and well positions. From Ohm et al. (2006).

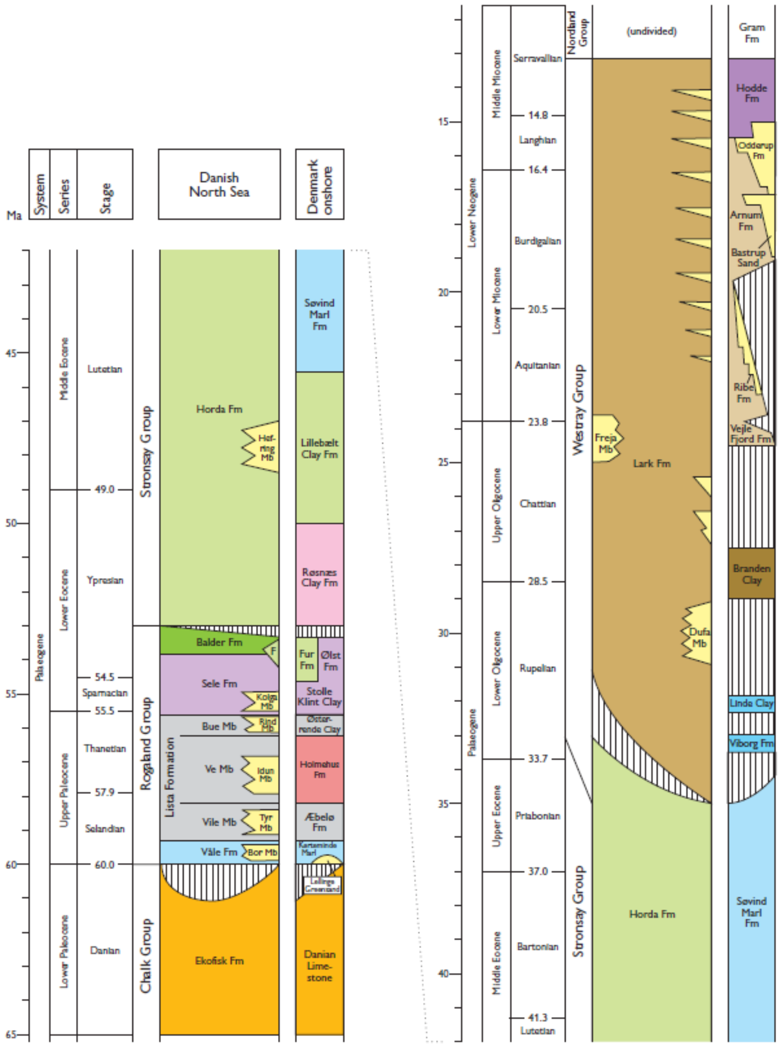

Figure 5 Lithostratigraphy scheme applied. From Schiøler et al. (2007).

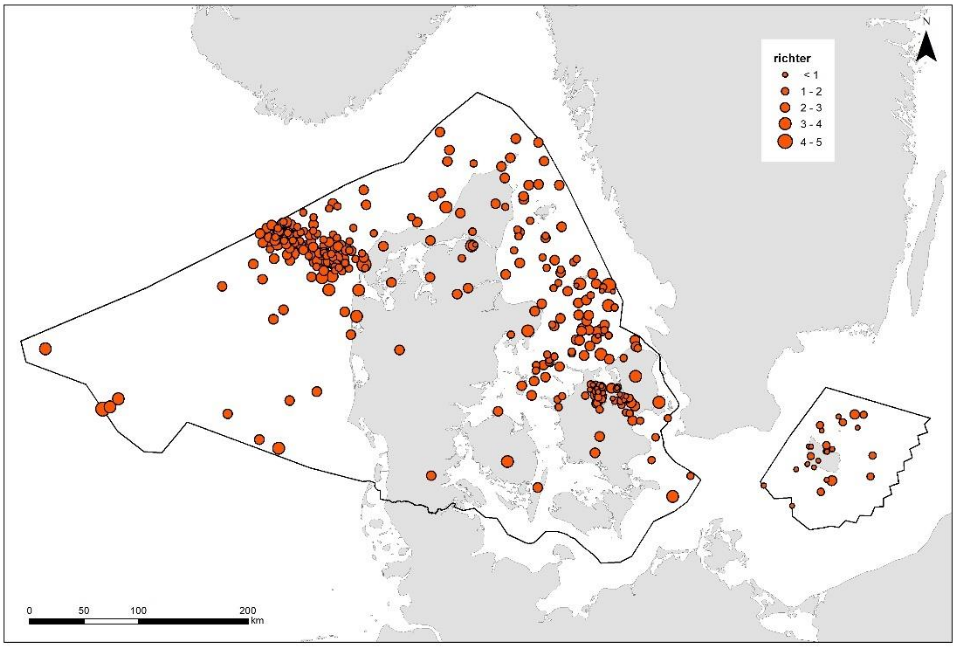

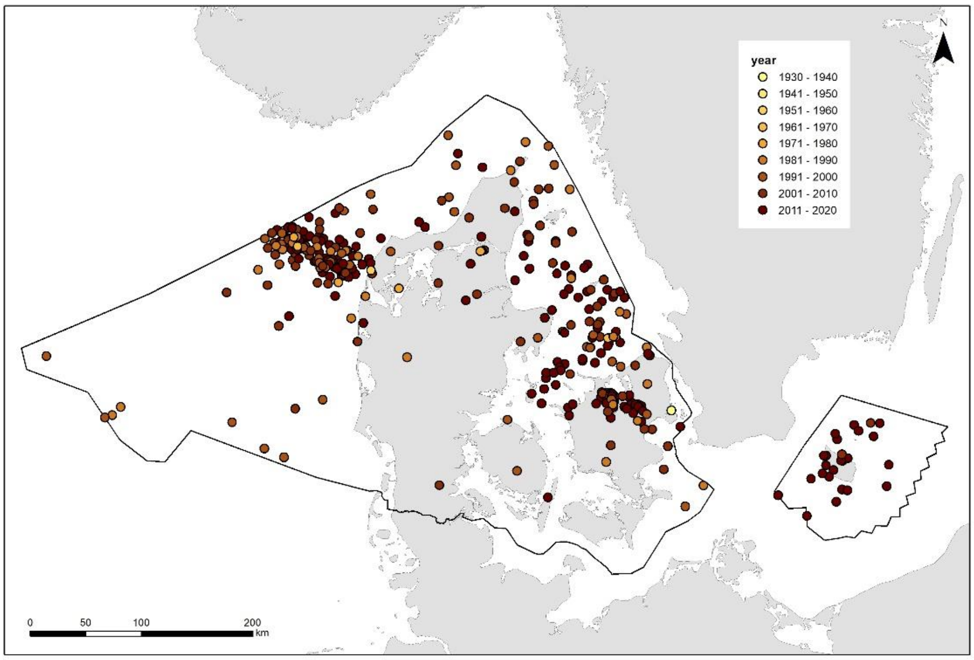

Figure 6 Total seismic activity recorded in Denmark on a minimum of three seismographs in the period 1930-10-31 to 2020-07-31. Upper figure show Richter scale and lower figure show time. Known detonations from the Navy and similar have been removed. Prepared by Tine Larsen (written communication 25 September 2020) from GEUS monitory depository. See also Jensen et al. (2013).

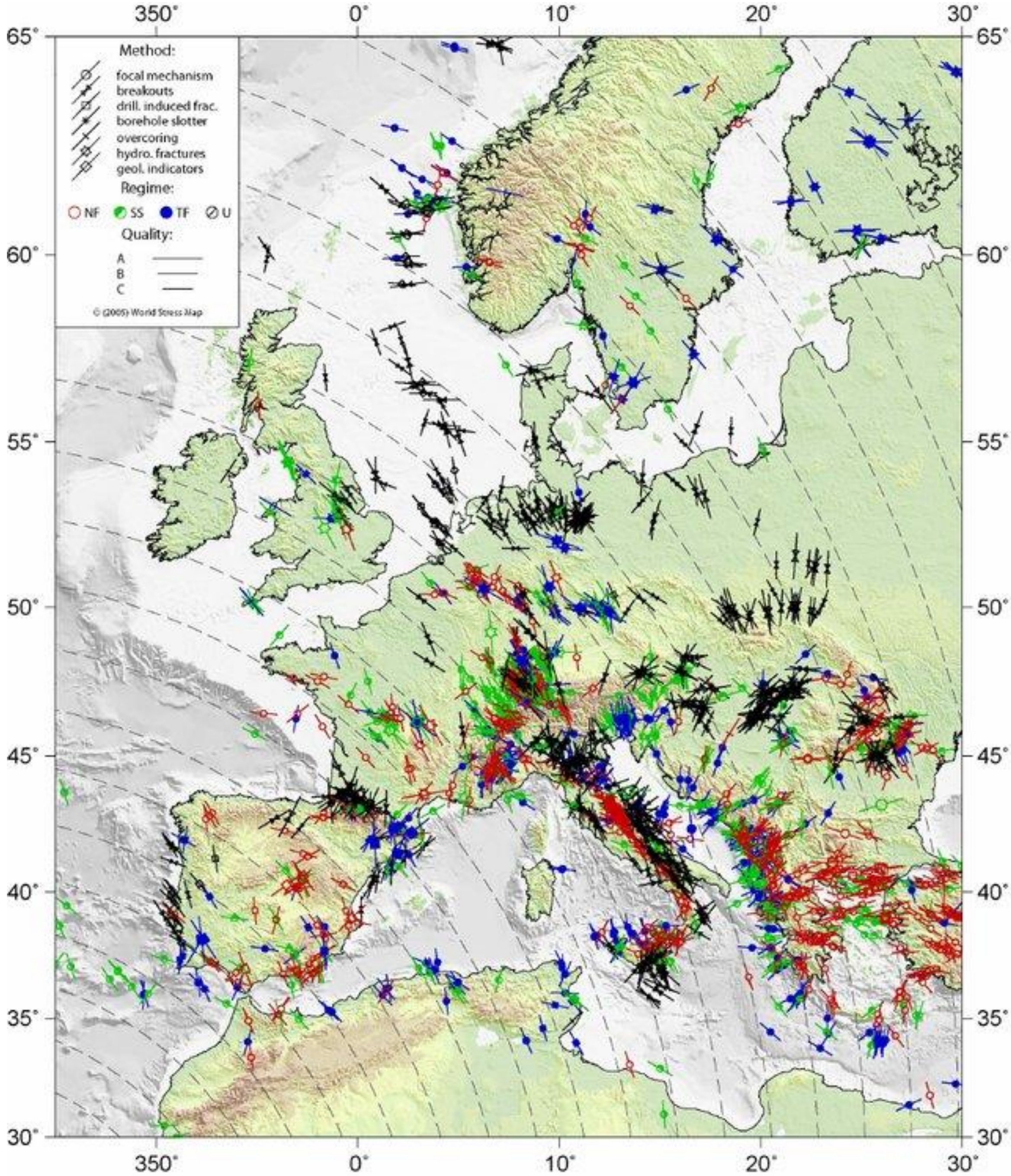

Figure 7 European stress map. Colours indicate stress regimes with red for normal faulting (NF), green for strike- slip faulting (SS), blue for thrust faulting (TF), and black for unknown regime (U). Lines represent the orientation of maximum horizontal compressional stress (S H), line length is proportional to quality. Grey lines are the trajectories of plate motion from Africa with respect to fixed Eurasia (Heidback et al. 2018). Available from http://www.world-stress-map.org/.

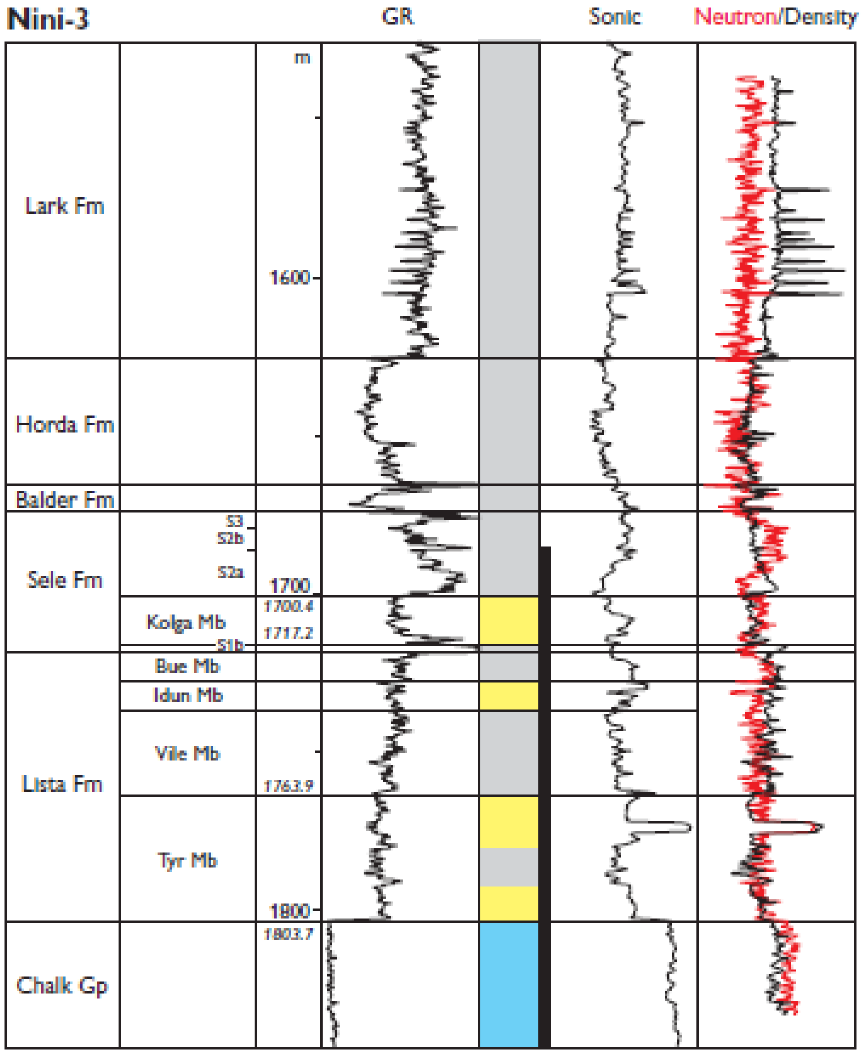

Figure 8 Stratigraphical division of the Nini-3 well. From Schiøler et al. (2007).

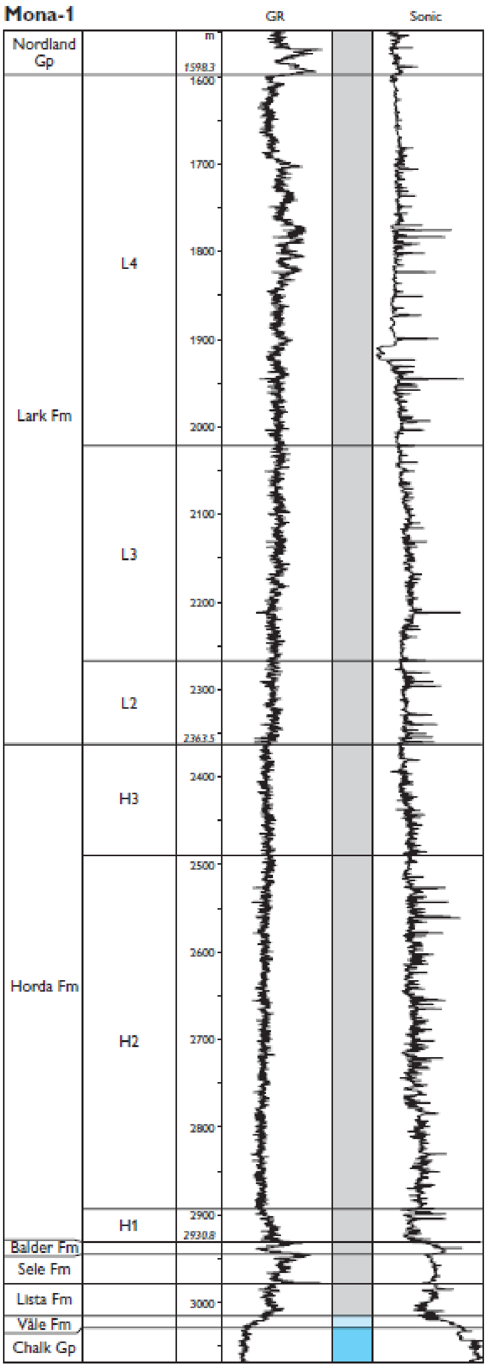

Figure 9 Mona-1, Danish reference well for the Horda and Lark Formations. The figure shows the tripartite subdivision of the Horda Formation and the L2–4 units of the Lark Formation. The L1 unit is absent in the Mona-1 area. From Schiøler et al. (2007).

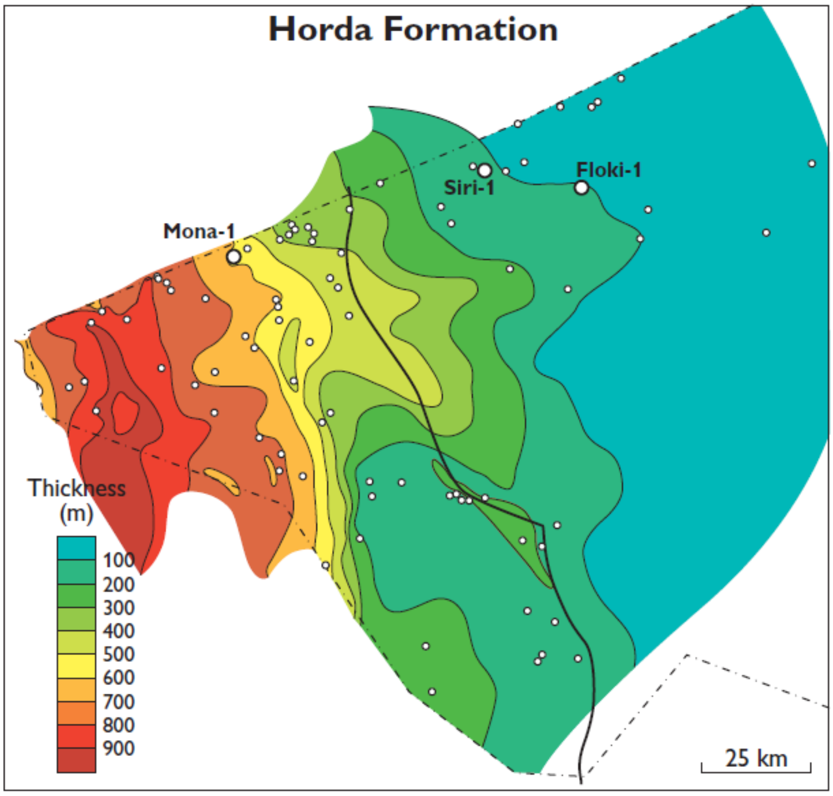

Figure 10 Isochore map of the Horda Formation. From Schiøler et al. (2007).

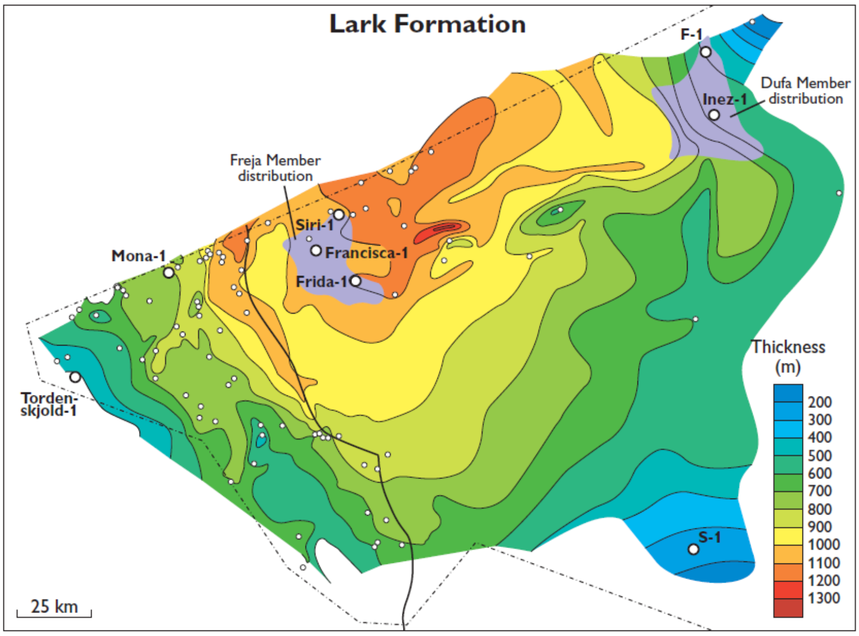

Figure 11 Isochore map of the Lark Formation. From Schiøler et al. (2007).

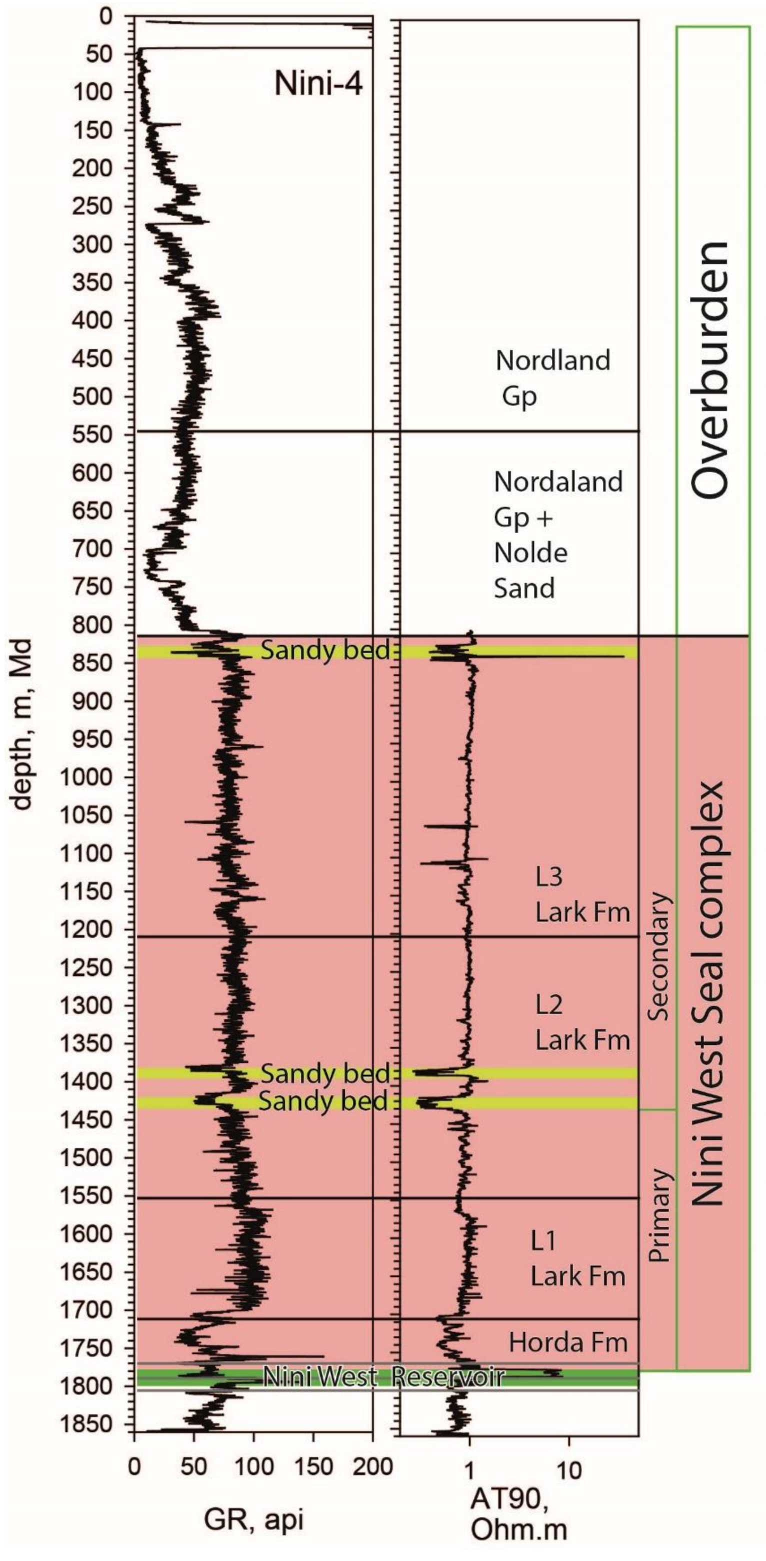

Figure 12 Seal and overburden units in the Nini-4 well.

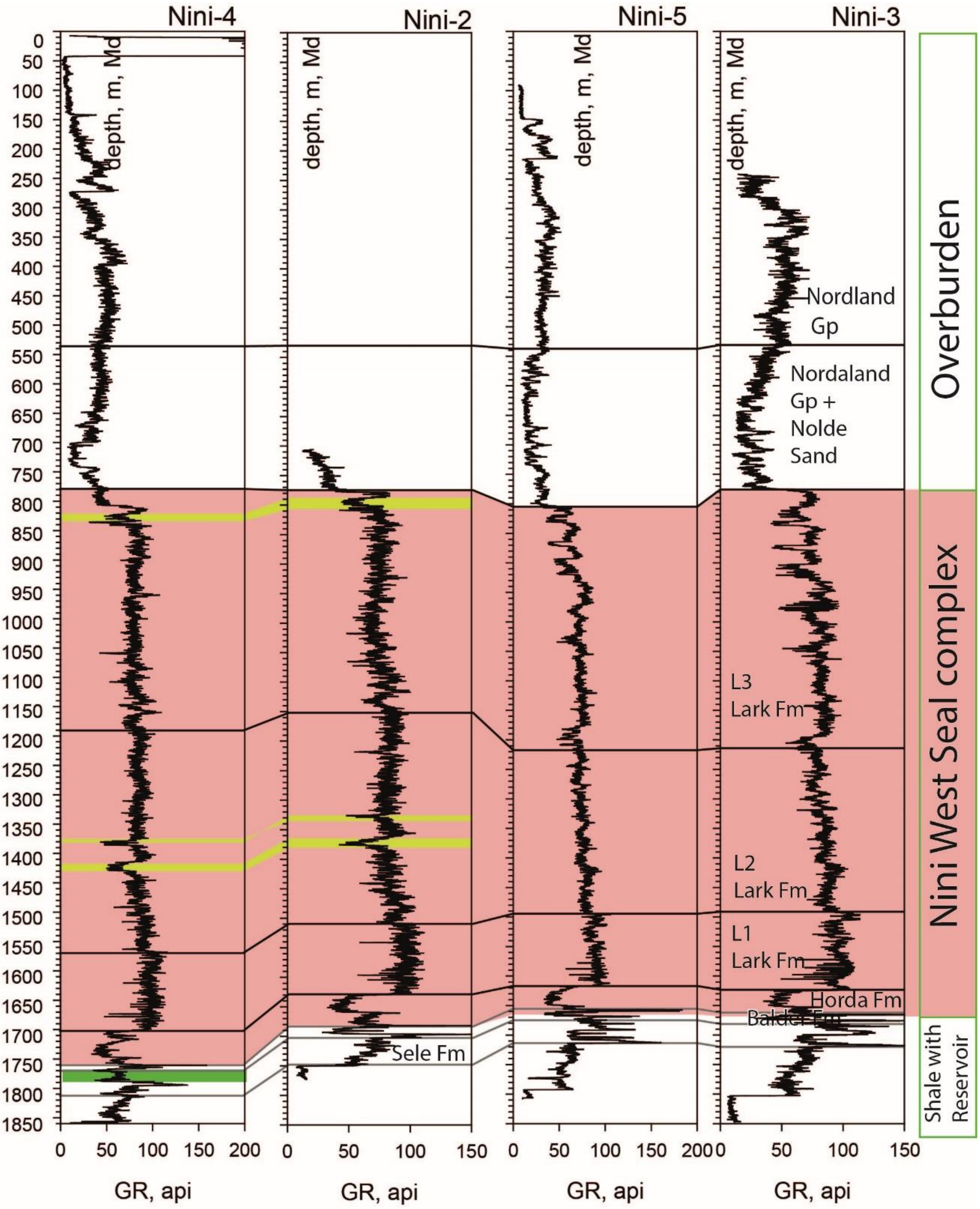

Figure 13 Well correlation across the Nini field complex (SW to NE) approximately 12 km. Well selected from vertical exploration wells. For location of wells see Fig. 4.

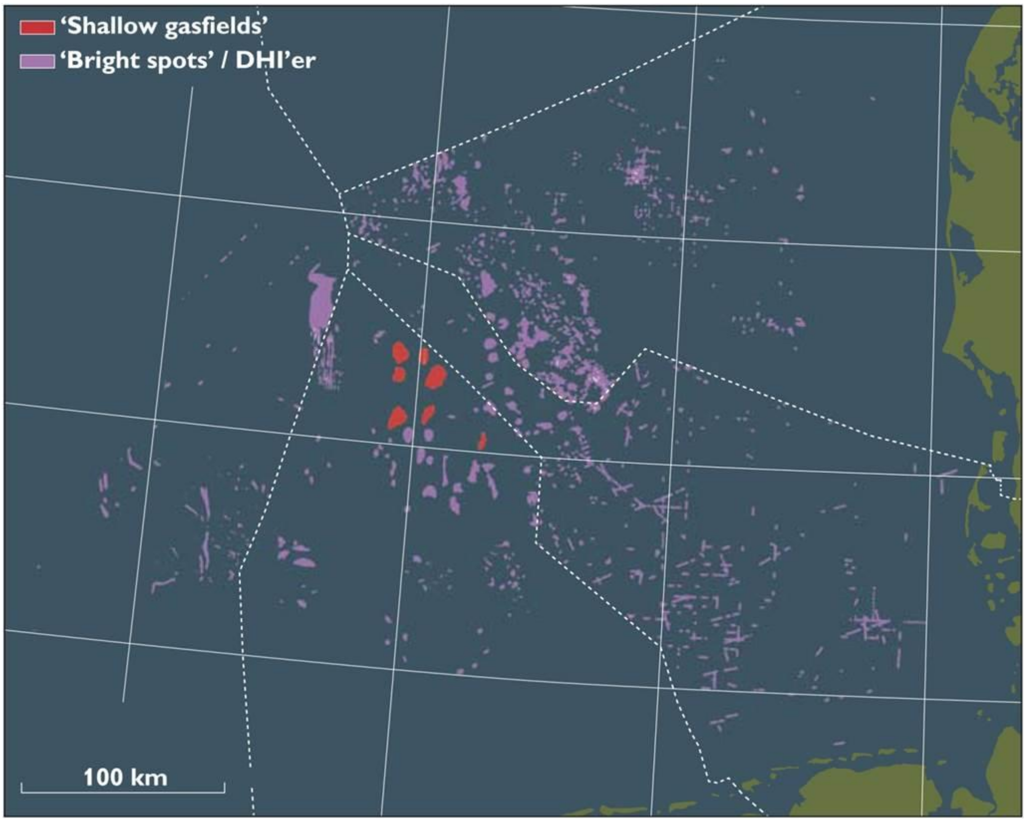

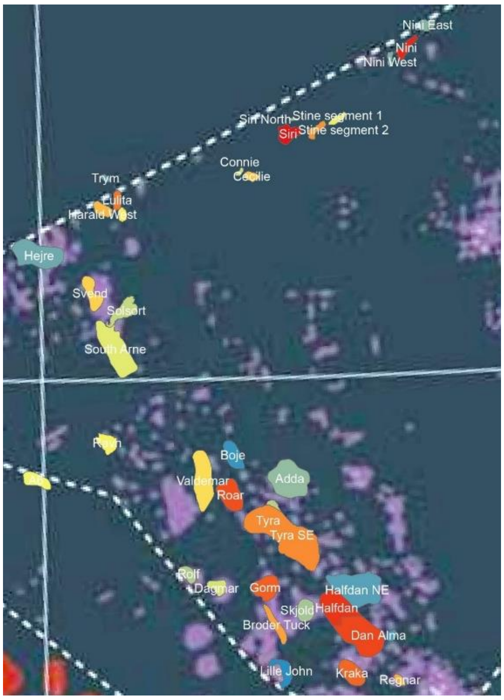

Figure 14 Bright spots in southern North Sea. Bright spots are indicative of presence of leaked gas in from oil and gas fields and/or of shallow biogenic gas. The Siri Canyon and the Nini Fields are located within an area of low bright spot activity (below). From Southern Permian Basin Atlas (https://www.nlog.nl/southern-permian-basin-atlas).

Figure 15 Horda Formation, primary seal in the Nini West. Core photos from the Nini-4 in interval 1760 – 1765 m.

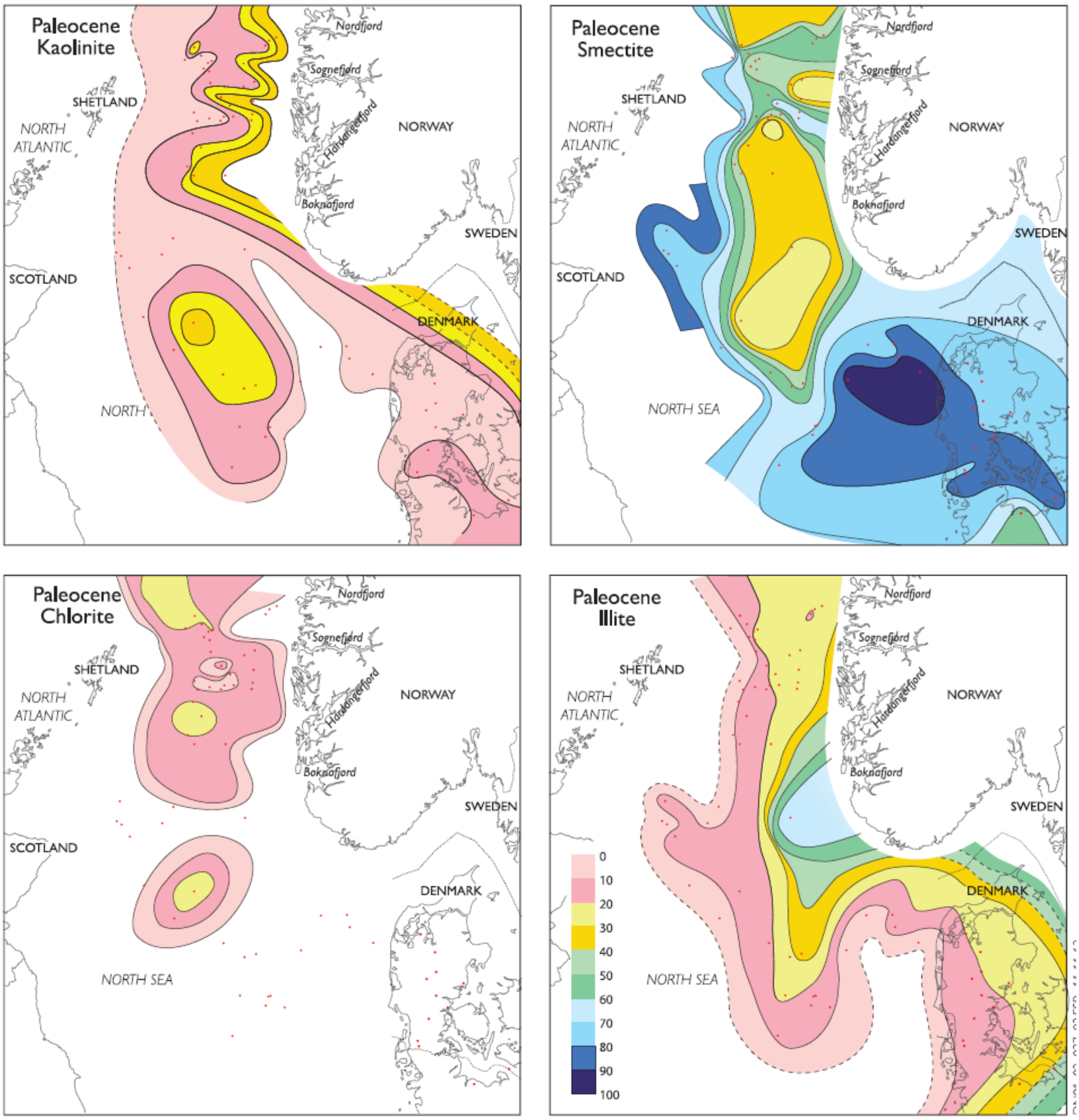

Figure 16 Distribution of minerals in the Palaeocene section. From Nielsen at al. (2015).

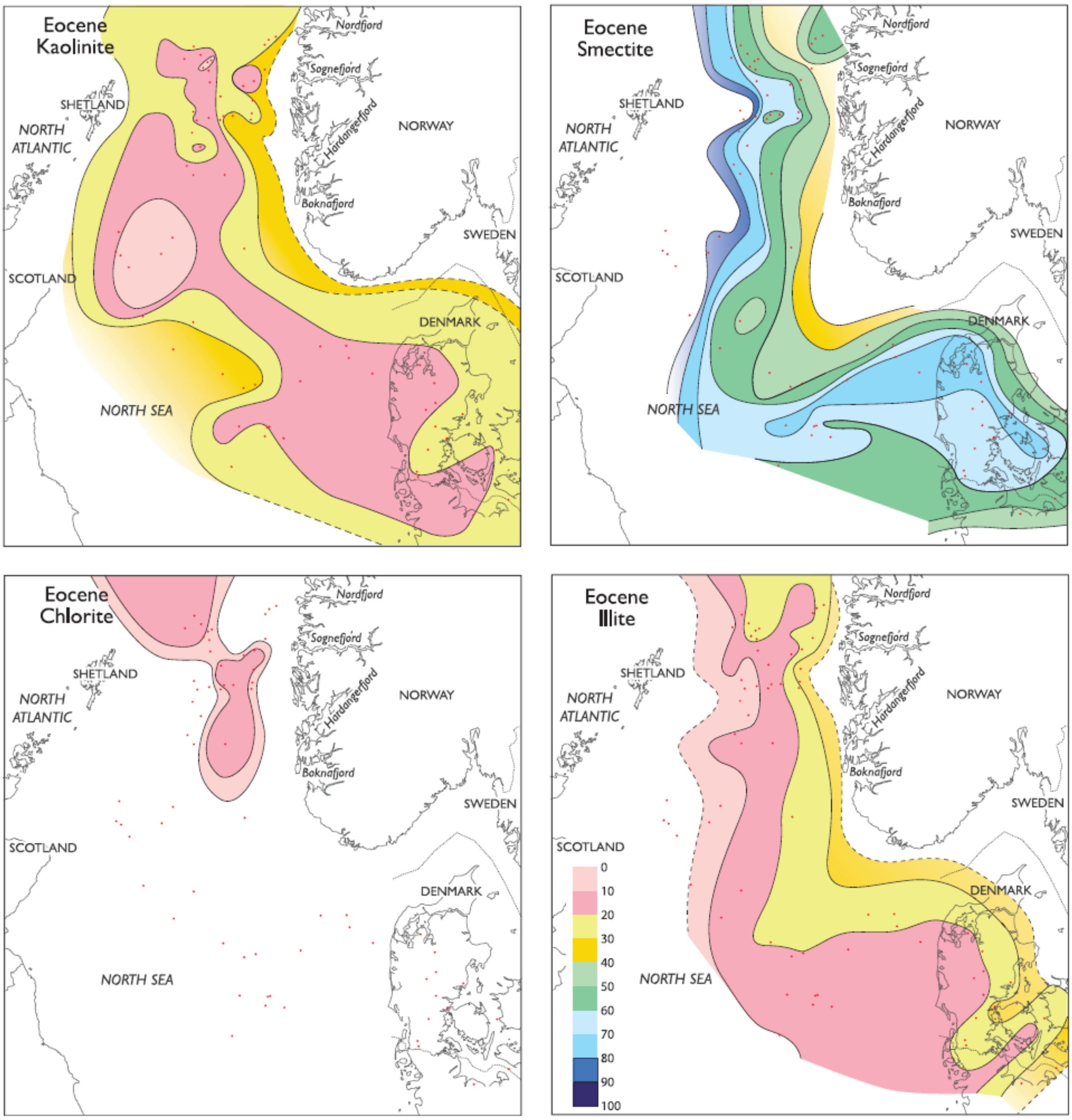

Figure 17 Distribution of minerals in the Eocene section. From Nielsen at al. (2015).

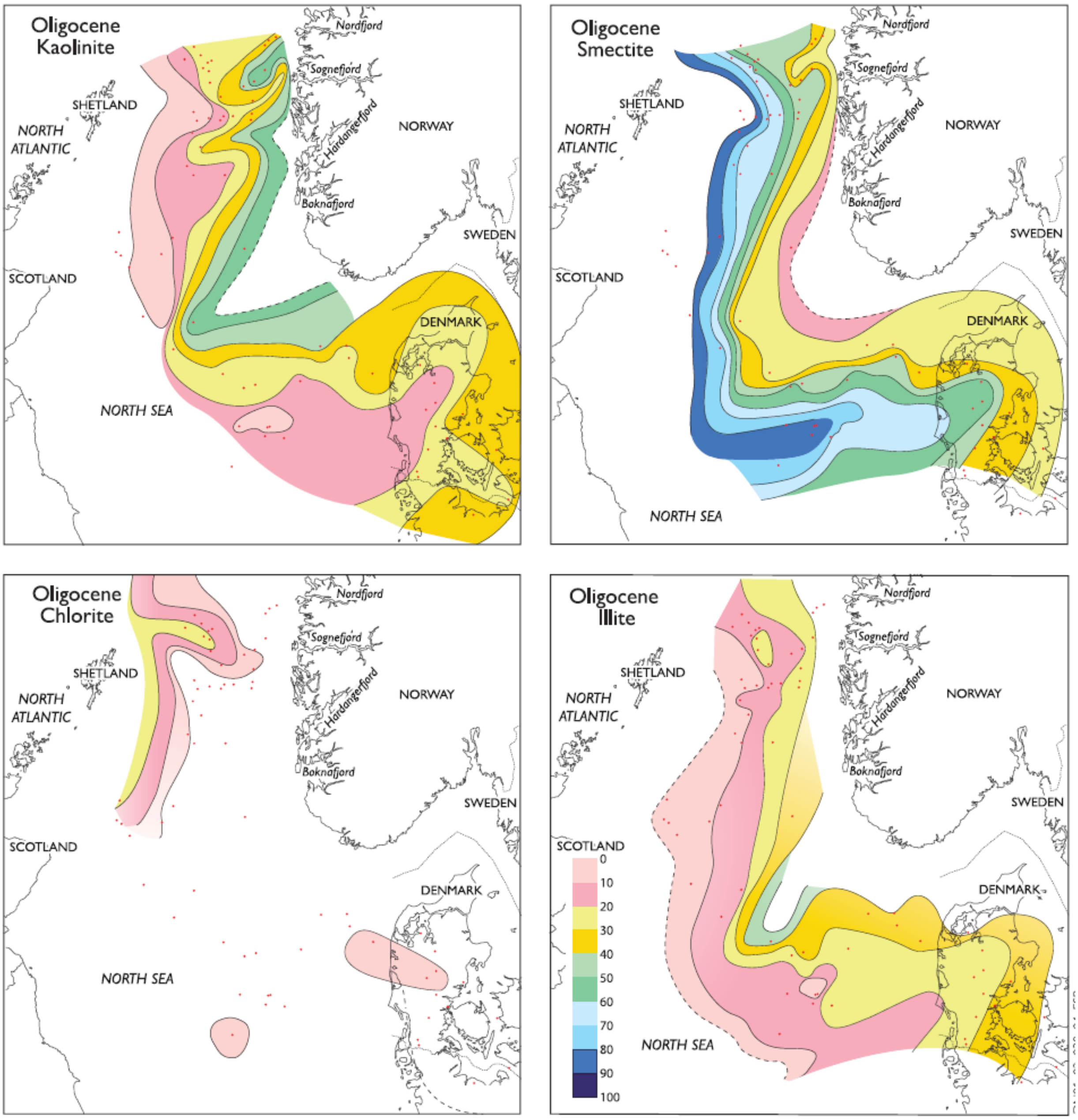

Figure 18 Distribution of minerals in the Oligocene section. From Nielsen at al. (2015).

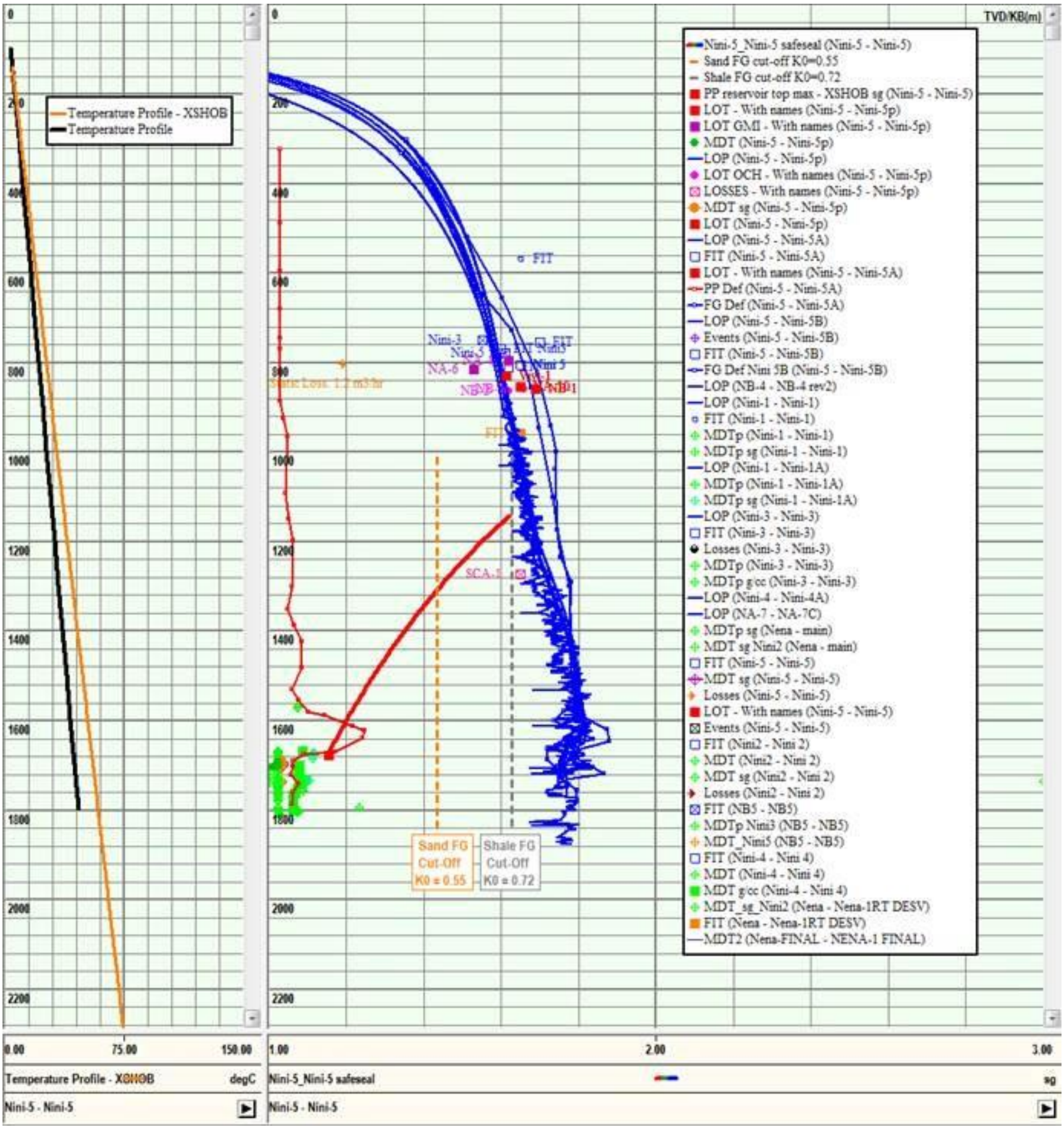

Figure 19 Leak of pressure and tests in the Nini-1 to -5 wells expressed in mud-weight equivalents (sg). Data compiled by INEOS and provided by Kent Johansen (written communication 30th August 2020).

Danish Ministry of Climate, Energy and Utilities

Geological survey of
Denmark and Greenland (GEUS)

Øster Voldgade 10
DK-1350 Copenhagen K
Denmark

GEUS is a research and advisory institution in the Danish Ministry of Climate, Energy and Utilities